MICROCOPY RESOLUTION TEST CHART

UNCLASSIFIED

~~CONFIDENTIAL~~ MOST Project -3

ADA036313

GENERAL ⓖ ELECTRIC

HEAVY MILITARY ELECTRONICS DEPARTMENT

TECHNICAL INFORMATION SERIES

AUTHOR	SUBJECT CATEGORY	NO. R65EMH13
J. P. Costas		DATE May 21, 1965

TITLE
SOME NOTES ON SONAR SYSTEM
AN/SQS-26 (XN-2) SEA DATA ANALYSIS. (U)

21 May 65

REPRODUCIBLE COPY FILED AT	G.E. CLASS 3	NO. PAGES
HMED Technical Publications Box 1122, FRP 1-5A Syracuse, New York 13201	GOVT. CLASS UNCLASSIFIED	53

59 p.

SUMMARY (unclassified)

The work reported continues the effort documented in TIS R64EMH22 and TIS R64EMH32. Extensive computer processing of sea returns has consistently revealed serious performance anomalies when particular modulation types are employed. An attempt to explain such negative results is undertaken by means of a computer simulation of both the active sonar system and the environment in which the system operates. Various combinations of modulation types and environmental parameters are tested and the simulation results are compared with results obtained in actual sea return processing.

The results obtained indicate that many of the anomalies observed in the processing of sea returns may be explained in terms of certain environmental or medium effects. It is further shown that a basic incompatibility can exist between modulation type and operating environment. Such mismatch can produce anomalies in the system displays and result in loss of detection capability.

DDC
RECEIVED
MAR 3 1977

(a)

GE³

HMED 4023A (5-65)

149510

~~CONFIDENTIAL~~

UNCLASSIFIED

GENERAL ELECTRIC COMPANY TECHNICAL INFORMATION

Within the limitations imposed by Government data export regulations and security classifications, the availability of General Electric Company technical information is regulated by the following classifications in order to safeguard proprietary information:

CLASS 1: <u>GENERAL INFORMATION</u>

> Available to anyone on request.
> Patent, legal and commercial review
> required before issue.

CLASS 2: <u>GENERAL COMPANY INFORMATION</u>

> Available to any General Electric Company
> employee on request.
> Available to any General Electric Subsidiary
> or Licensee sugject to existing agreements.
> Disclosure outside General Electric Company
> requires approval of originating component.

CLASS 3: <u>LIMITED AVAILABILITY INFORMATION</u>

> Original Distribution to those individuals with
> specific need for information.
> Subsequent Company availability requires
> originating component approval.
> Disclosure outside General Electric Company
> requires approval of originating component.

CLASS 4: <u>HIGHLY RESTRICTED DISTRIBUTION</u>

> Original distribution to those individuals person-
> ally responsible for the Company's interests in
> the subject.
> Copies serially numbered, assigned and recorded
> by name.
> Material content, and knowledge of existence,
> restricted to copy holder.

GOVERNMENT SECURITY CLASSIFICATIONS, when required, take precedence in the handling of the material. Wherever not specifically disallowed, the General Electric classifications should also be included in order to obtain proper handling routines.

SECTION __Advance Projects Development Operation__

UNIT _____

HMED ACCOUNTING REFERENCE __572__

COLLABORATORS _____

APPROVED __Mayn A. Johnson__ TITLE __Manager__ LOCATION __CSP 4-4, Syracuse__

TIS R65EMH13

MINIMUM DISTRIBUTION - <u>Government Unclassified</u> Material (and Title Pages) in G.E. Classes 1, 2, or 3 will be the following.

Copies	Title Page Only	To
0	1	Legal Section, HMED (Syracuse)
1	0	Manager, Technological Planning, HMED (Syracuse)
1	1	Electronics Park Library (Syracuse)
2	6	G.E. Technical Data Center (Schenectady)

MINIMUM DISTRIBUTION - <u>Government Classified</u> Material, Secret or Confidential in G.E. Classes 1, 2, or 3 will be the following.

1	1	Classified Section, Electronics Park Library.

ADDITIONAL DISTRIBUTION (Keep at minimum within intent of assigned G.E. Class.)

COPIES	NAME	LOCATION
4	Astemborski, T.J.	FRP 1-122A, Syracuse, New York
1	Burkart, H.H.	FRP 1-73, Syracuse, New York
10	Costas, J.P.	CSP 4-4, Syracuse, New York
1	Donegan, J.H.	FRP 1-122A, Syracuse, New York
1	Edward, J.A.	FRP 1-122A, Syracuse, New York
11	Garber, S.M.	FRP 1-122A, Syracuse, New York
1	Janer, R.	CSP 4-16, Syracuse, New York
1	Latimer, H.B.	CSP 9-3, Syracuse, New York
1	McNeill, J.F.	CSP 3-3, Syracuse, New York
1	Nardello, J.P.	FRP 1-122A, Syracuse, New York
1	Nasipak, V.	FRP 1-30, Syracuse, New York
1	Poorman, W.W.	CSP 3-3, Syracuse, New York
1	Pratt, J.R.	FRP 1-77, Syracuse, New York
1	Stutt, C.A./ Shuey, R.L. Drs.	Research Laboratory, Schenectady, New York
1	Stark, M.	CSP 4-16, Syracuse, New York
1	Sweetman, R.	FRP 1-73, Syracuse, New York

HMED 4024 (5-65)

~~CONFIDENTIAL~~

TABLE OF CONTENTS

D D C

RECEIVED

MAR 3 1977

D

~~CONFIDENTIAL~~

i

LIST OF ILLUSTRATIONS

LIST OF ILLUSTRATIONS (Continued)

SOME NOTES ON SONAR SYSTEM AN/SQS-26 (XN-2) SEA DATA ANALYSIS
TIS R65EMH13

I. INTRODUCTION

In a previous report, coauthored by the present writer and L. W. Bauer,*
an extensive analysis of selected sonar returns was performed. This report
(R65EMH13) may be considered as a sequel to the previous report. Statements
made here which are derived from the earlier report are keyed with an asterisk (*).
It is necessary that the reader review that report, since a great deal of
explanatory detail contained there has been omitted here.

Two types of signal processors were employed in the analysis of sonar sea
data.* The first type of processor was a very crude, noncoherent IF processor
which performed a square-law detection of the IF signal, followed by an integrating
or smoothing baseband filter. This processor, for rather obvious reasons, was
called a power detector, and all of the 391 pings available on the digital tapes
were power-detector processed. A much more sophisticated type of signal processor
was also simulated on the IBM 7094 computer; 23 sea returns and three test returns
were processed by this second means. This second type of processing consisted of
ideal (analog) correlation detection of the received pings, followed by ideal
filtering of the correlator output. The post-correlator filters consisted of a
theoretically-optimum bank of doppler filters, the detected outputs of which were
presented by means of range-velocity indicator (RVI) displays.

By means of the second processor simulation described above, a rather complete
"picture" of the sea returns could be obtained. The RVI displays, presented for
various values of threshold setting, describe the behavior of the sea returns in
both the time and frequency domains. Such computer simulation eliminates the
possibility of performance degradation due to practical hardware limitations; for
example, performance degradation caused by the Deltic correlator in actual
AN/SQS-26 signal processing is eliminated as a possible cause for concern. The
"ideal" signal processor lineup simulated* would be most difficult and extremely
expensive to duplicate in practice.

---

*Computer Analysis of Sonar System AN/SQS-26 (XN-2) Sea Data, TIS R64EMH32,
General Electric Company, Syracuse, New York, October 29, 1964.

The analog-correlation processor considered* was far more sophisticated than the power detector, yet a comparison of sea data analysis results was hardly encouraging; in many cases it was quite evident that the simple power detector provided a much better means for the detection of sonar targets than did the sophisticated "ideal" processor. The disappointing results obtained with the analog-correlation processor motivated this present memorandum, which reports the results of some additional work performed in an attempt to explain the disturbing results which had been obtained in the previous study effort.

Three types of modulation were employed in the previous report: linear frequency modulation (FM), pseudo-random noise (PRN), and random frequency modulation (RFM). From the point of view of a simple detection it was clear that FM gave by far the best performance; however, for this type of modulation, the elaborate RVI presentations are somewhat redundant since this type of waveform does not permit target range and velocity information to be resolved. The PRN and RFM waveforms were known to have "thumbtack" ambiguity surfaces; it was hoped that these two waveforms would yield RVI displays which would not only show the presence of the target but would also indicate the true velocity and true range of the target submarine. The performance of these latter two waveforms, with very few exceptions, did not meet expectations. Detectability was not as good as in the case of FM and, with regard to range and doppler information, the RVI displays were most disappointing. This is a serious situation, since much of the present AN/SQS-26 system design and many future applications of this sonar system are predicated on the assumption that accurate range and doppler information will be derived from the received waveform. The results of the previous report give strong indications that, not only is such accurate range and doppler information unavailable, but that attempts to obtain this information can result in a serious loss in detectability. Quite obviously, such results are significant and it was felt that further investigations were in order.

The work reported in this memorandum was undertaken in an effort to obtain some plausible explanation for the negative results obtained with the sea data. Computer simulation techniques are again employed, but actual sea returns are not used, rather the sonar signal processing system and the inputs to this system are entirely simulated. In this manner controlled and known input conditions may be created which, of course, enable a much more accurate evaluation of the signal processor output results.

II. WAVEFORM ANALYSIS

In a system as complex as the AN/SQS-26 there are many possible problem areas. One item of some concern is the quality of the waveforms actually put into the water by the system. The sea tapes processed* contain "test returns" which are actually recordings made at hydrophone terminals during the transmit period in the system cycle. These test returns are given numbers; e.g., ping 123 (FM), ping 294 (PRN), and ping 29 (RFM). The analysis of this particular set of test returns may be found in the previous report on pages 43 through 59.

FM ping 123 shows RVI displays of the type that are expected for this type of modulation. The ambiguity surface is a ridge, and the volume under the ambiguity surface is well-confined to the ridge region (Figures 13 through 17*). This result is precisely what would be expected from theoretical considerations.

The PRN test return, ping 294, gives RVI displays which are again consistent with theory (Figures 19 through 21*). It was noted that the threshold could be lowered, in this case to 9 db below the peak, before range-doppler sidelobes made their appearance. The 12- and 15-db thresholds showed considerable range-doppler sidelobe activity, but this is not too surprising for such a waveform. Since the bandwidth of this pulse is 100 cycles and its duration is one-half second, crude theory would indicate that the close-in sidelobe level should be on the average at -20 db relative to the peak; however, the 2BT factor obtained from theory with regard to the ambiguity surface is an average value -- this certainly does not preclude sidelobe peaks from appearing well above this level. Thus, the results obtained* for this test return appear to be in reasonable agreement with theoretical expectations.

The behavior of the RFM test return, ping 29 (Figures 23 through 25*) is very much like that of the PRN ping. Very little range-doppler sidelobe activity is evident at the 9-db level, while considerable activity is seen at the 12-db threshold setting (Figure 24*). Here again, these results agree closely with what might be expected from a theoretical analysis of the ambiguity properties of such a waveform.

In spite of the reasonable agreement between the test return RVI displays* and theory, it was decided that additional tests should be performed using complete simulation techniques. Computer programs were written to generate the above three

types of waveforms, and simulation programming was also done so that the ambiguity surface of the simulated waveforms could be determined by means of RVI displays. The first waveform tested by this method was of the FM type; the parameters used are shown in Table 1, and the results are shown in Figures 1, 2, and 3. The RVI display for a 3-db threshold is shown in Figure 1. The vertical scale indicates doppler setting in knots; the horizontal scale indicates time or range in seconds. A total of 61 filters are employed in the simulated processor, with a center-frequency spacing of 0.8 knot and a bandwidth consistent with the 0.5-second pulse duration. The characteristic ridge line which is associated with this type of modulation may be seen in Figure 1. The breaks in this curve are apparently caused by the "crossover-dip" of the filter bank design. This may be further confirmed by noting the double response in two regions which occur in Figure 2 -- the RVI display for a 6-db threshold setting. Figures 3, 4, and 5 show the performance of this waveform as the threshold setting is lowered in 3-db steps to 15 db. This performance is characteristic of FM and agrees very well with the results obtained* for the FM test return, ping 123. (There are some differences between the RVI displays of the previous report and this memorandum since the range or time scales are different.)

The ambiguity surface for PRN modulation is shown in Figures 6 through 10; the parameters employed are shown in Table 2. The figures indicate that, for this waveform, range-doppler sidelobe activity does not make an appearance until the threshold is lowered to about 12 db below the central peak. At a 15-db threshold, considerable range-doppler sidelobe activity is to be noted (see Figure 10); these results compare favorably with those found previously (Figures 19 through 21*). Figure 20* does indicate some sidelobe activity at the 9-db level which is not shown in Figure 6; however, this difference appears to be minor and not particularly significant. It is interesting to note that a central-point symmetry exists in the RVI displays which is consistent with the theory of the ambiguity function.

The simulation results for the RFM waveform are shown in Figures 11 through 15; the parameters employed are shown in Table 3. It will be noted that sidelobe activity does not appear until the threshold is lowered to 12 db, and that considerable sidelobe activity is to be noticed at the 15-db threshold setting (Figure 15). Here again, central-point symmetry is clearly in evidence. Comparing Figures 11 through 15 with Figures 23* through 25* shows very good agreement with

regard to sidelobe level. Very little sidelobe activity was noted at the 9-db threshold setting (Figure 24*), and one might conclude that somewhat better agreement between simulation and actual test return processing is obtained for RFM as compared to PRN; however, the agreement in all cases is sufficiently good that there may be rasonable confidence in the quality of the signals put into the water by the AN/SQS-26 system. Put another way, the simulation results that have just been described give no indication of any serious differences compared to the waveforms generated by the AN/SQS-26 system.

TABLE 1

SYSTEM PARAMETERS	
SYSTEM BANDWIDTH (CPS)	150.000000
SIGNAL BANDWIDTH (CPS)	100.000000
CARRIER FREQUENCY (CPS)	3400.000000
DOPPLER FILTER SETTING (KTS)	0.
INITIAL TIME SEARCH (SEC)	0.260000
FINAL TIME SEARCH (SEC)	0.740000
INITIAL TIME SEARCH INDEX	261
FINAL TIME SEARCH INDEX	741
TIME INCREMENT (SEC)	0.001000
SAMPLING RATIO	6.666667
PROPAGATION VELOCITY (KTS)	2900.000000
WAVEFORM TYPE	1
PULSE LENGTH (SEC)	0.500000

NOISE PARAMETERS	
INITIAL RANDOM NUMBER	106721074235
FINAL RANDOM NUMBER	106721074235
NUMBER NOISE TERMS USED	265
NUMBER NOISE SAMPLES USED	1503
AVERAGE POWER CALCULATED	0.

REFERENCE PARAMETERS	
NUMBER SAMPLE POINTS	501
INITIAL RANDOM NUMBER	123331725215
FINAL RANDOM NUMBER	123331725215
NUMBER NOISE TERMS USED	90

SIGNAL PARAMETERS

NO. TARGETS USED= 1   REFERENCE TARGET POWER= 0.10020E 01

TARGET	TIME	INDEX	POWER
1	0.5000	501	1.0000

(ALL RETURNS AT   0.   KNOTS)

RANGE-VELOCITY DISPLAY DATA

SAMPLING RATE   1000.00/SEC   DISPLAY INDEX   10   PEAK VOLTAGE 0.71134E 00   DOP. OF PEAK -0.000 KTS
TIME OF PEAK 0.50000E-00 SEC
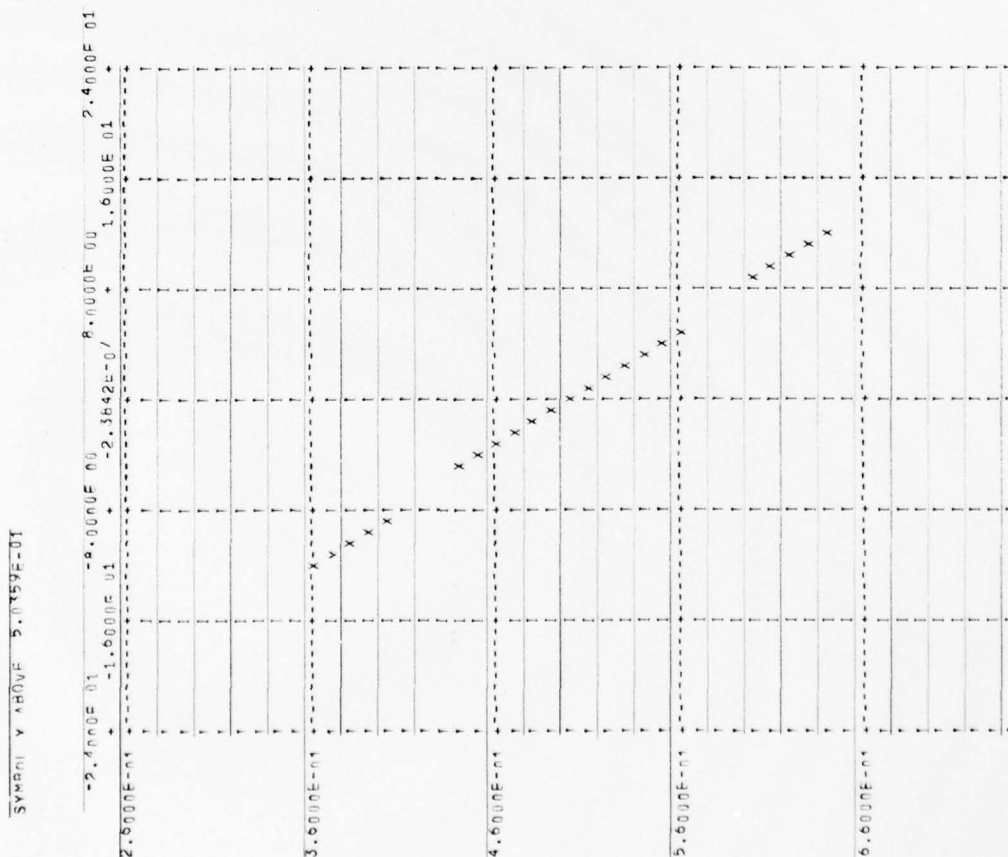
Figure 1.   RVI Display, FM, 3-db Threshold
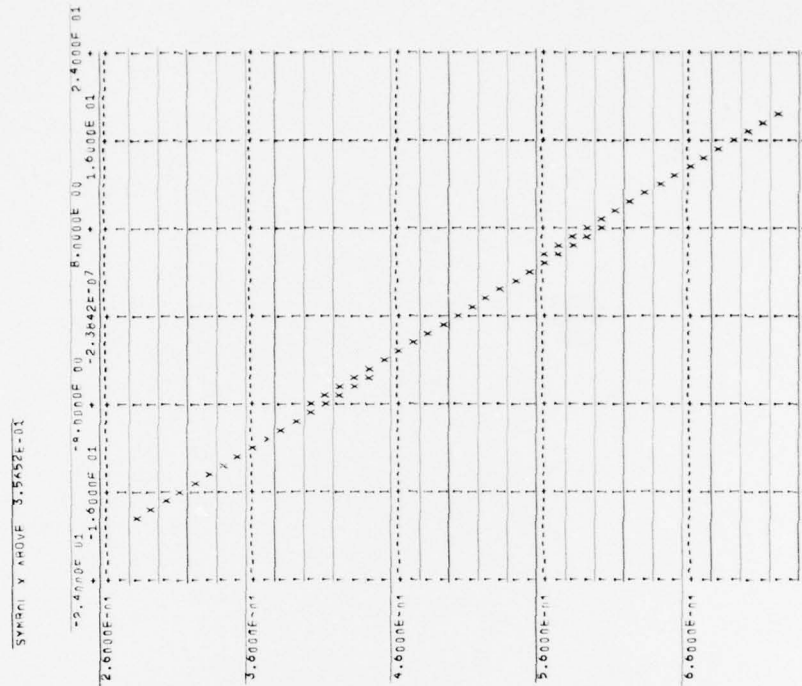
Figure 2.   RVI Display, FM, 6-db Threshold
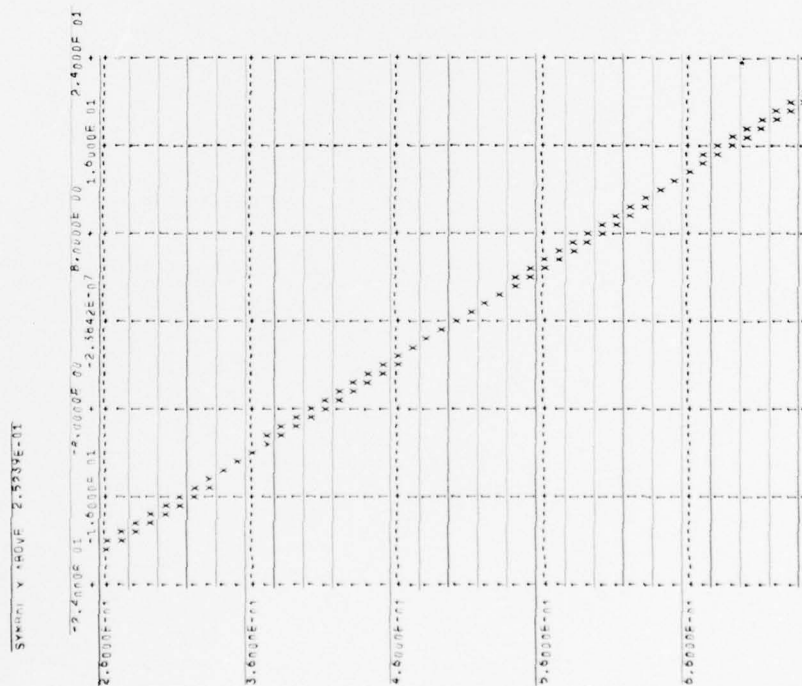
Figure 3.   RVI Display, FM, 9-db Threshold

7
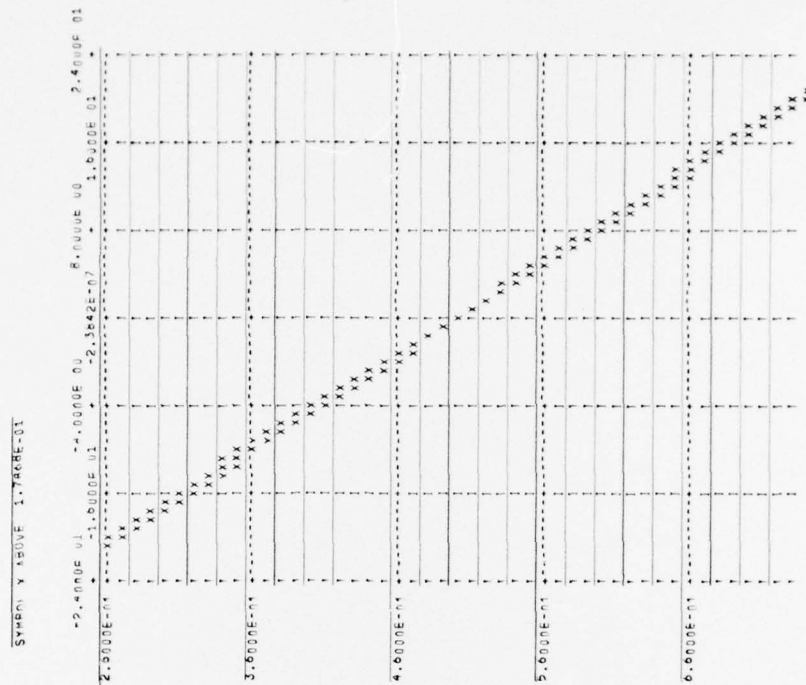
Figure 4. RVI Display, FM, 12-db Threshold
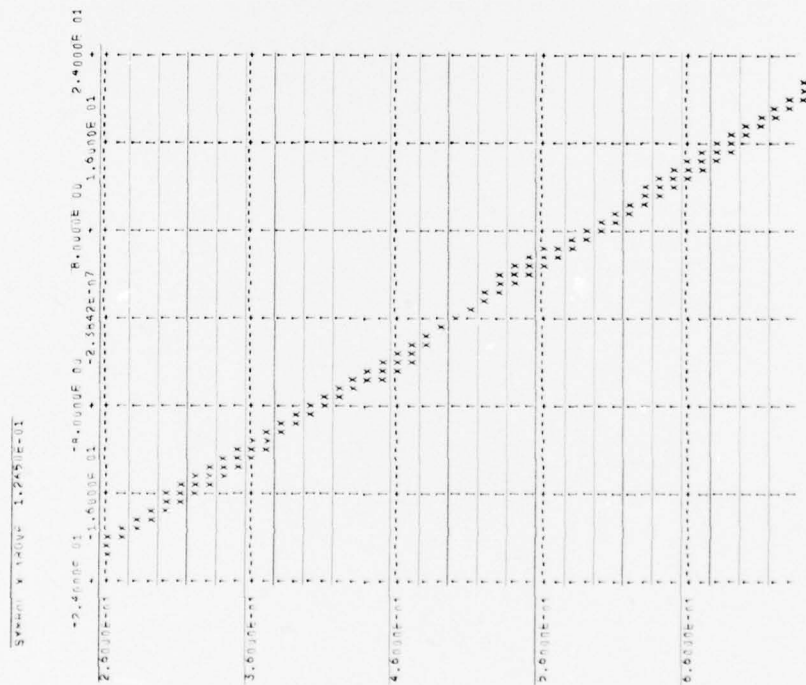
Figure 5. RVI Display, FM, 15-db Threshold

8

TABLE 2

SYSTEM PARAMETERS	
SYSTEM BANDWIDTH (CPS)	150.000000
SIGNAL BANDWIDTH (CPS)	100.000000
CARRIER FREQUENCY (CPS)	3400.000000
DOPPLER FILTER SETTING (KTS)	0.
INITIAL TIME SEARCH (SEC)	0.260000
FINAL TIME SEARCH (SEC)	0.740000
INITIAL TIME SEARCH INDEX	261
FINAL TIME SEARCH INDEX	741
TIME INCREMENT (SEC)	0.001000
SAMPLING RATIO	0.666667
PROPAGATION VELOCITY (KTS)	2900.000000
WAVEFORM TYPE	3
PULSE LENGTH (SEC)	0.500000

NOISE PARAMETERS	
INITIAL RANDOM NUMBER	106721074235
FINAL RANDOM NUMBER	106721074235
NUMBER NOISE TERMS USED	265
NUMBER NOISE SAMPLES USED	1503
AVERAGE POWER CALCULATED	0.

REFERENCE PARAMETERS	
NUMBER SAMPLE POINTS	501
INITIAL RANDOM NUMBER	123331725215
FINAL RANDOM NUMBER	005701402765
NUMBER NOISE TERMS USED	90

SIGNAL PARAMETERS

NO. TARGETS USED= 1   REFERENCE TARGET POWER= 0.10499E 01

TARGET	TIME	INDEX	POWER
1	0.5000	501	1.0000

(ALL RETURNS AT 0. KNOTS)

RANGE-VELOCITY DISPLAY DATA

SAMPLING RATE 1000.00/SEC   DISPLAY INDEX 10   PEAK VOLTAGE 0.10524E 01   DOP. OF PEAK -0.000 KTS
TIME OF PEAK 0.50000E-00 SEC

Figure 6.   RVI Display, PRN, 3-db Threshold
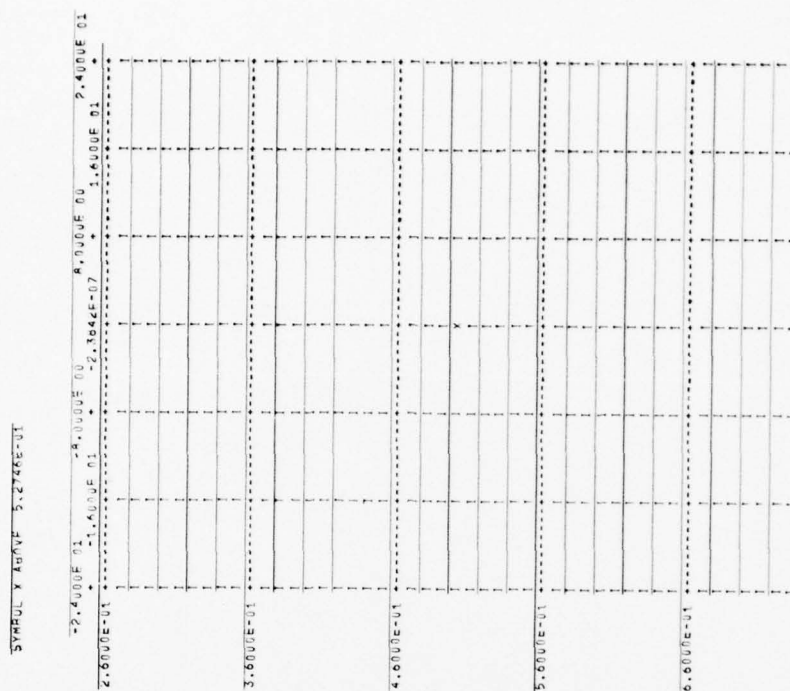
Figure 7.   RVI Display, PRN, 6-db Threshold
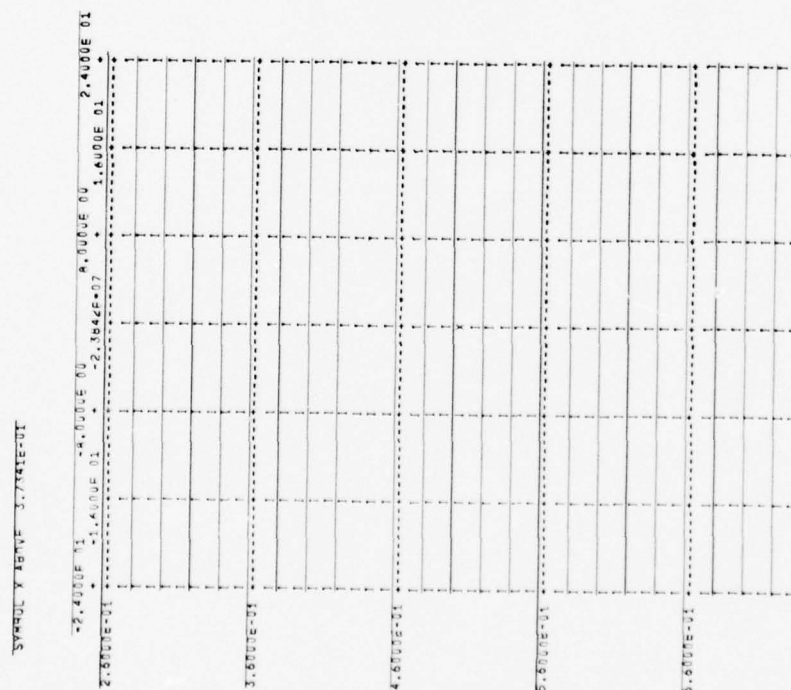
Figure 8.   RVI Display, PRN, 9-db Threshold
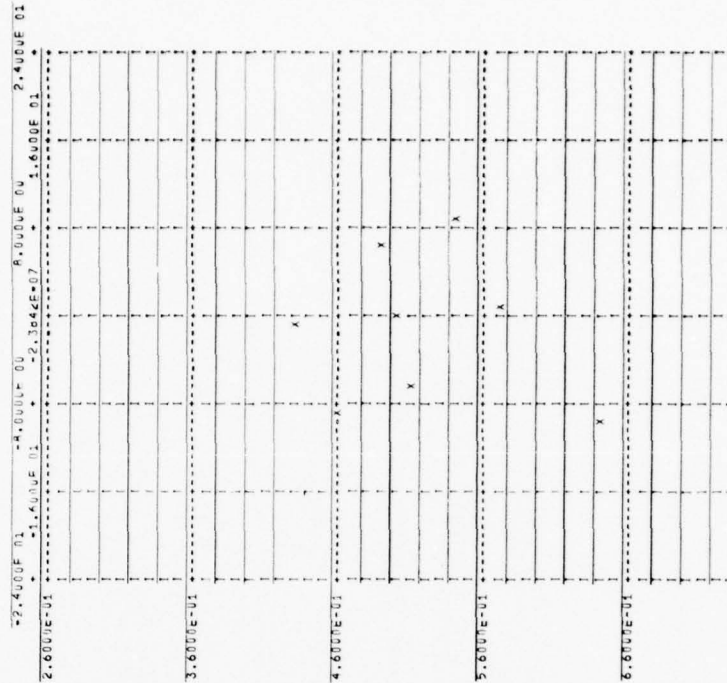
Figure 9.   RVI Display, PRN, 12-db Threshold
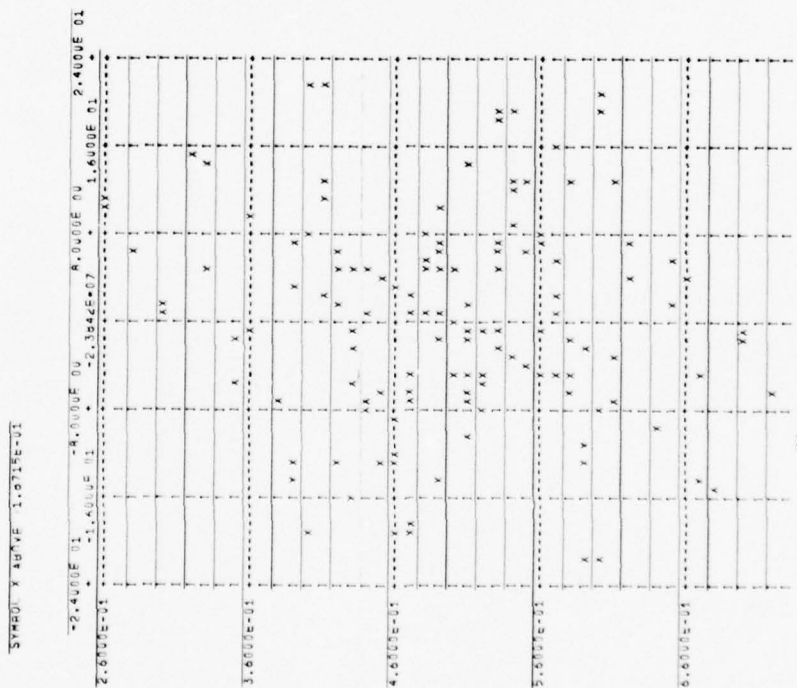
Figure 10.   RVI Display, PRN, 15-db Threshold

TABLE 3

SYSTEM PARAMETERS	
SYSTEM BANDWIDTH (CPS)	150.000000
SIGNAL BANDWIDTH (CPS)	100.000000
CARRIER FREQUENCY (CPS)	3400.000000
DOPPLER FILTER SETTING (KTS)	0.
INITIAL TIME SEARCH (SEC)	0.260000
FINAL TIME SEARCH (SEC)	0.740000
INITIAL TIME SEARCH INDEX	261
FINAL TIME SEARCH INDEX	741
TIME INCREMENT (SEC)	0.001000
SAMPLING RATIO	6.666667
PROPAGATION VELOCITY (KTS)	2900.000000
WAVEFORM TYPE	4
PULSE LENGTH (SEC)	0.500000

NOISE PARAMETERS	
INITIAL RANDOM NUMBER	106721074235
FINAL RANDOM NUMBER	106721074235
NUMBER NOISE TERMS USED	265
NUMBER NOISE SAMPLES USED	1503
AVERAGE POWER CALCULATED	0.

REFERENCE PARAMETERS	
NUMBER SAMPLE POINTS	501
INITIAL RANDOM NUMBER	123331725215
FINAL RANDOM NUMBER	123331725215
NUMBER NOISE TERMS USED	90

SIGNAL PARAMETERS

NO. TARGETS USED= 1   REFERENCE TARGET POWER= 0.99989E 00

TARGET	TIME	INDEX	POWER
1	0.5000	501	1.0000

(ALL RETURNS AT   0.   KNOTS)

RANGE-VELOCITY DISPLAY DATA

SAMPLING RATE   1000.00/SEC   DISPLAY INDEX   10   PEAK VOLTAGE 0.70952E 00   DOP. OF PEAK -0.000 KTS
TIME OF PEAK 0.50000E-00 SEC

Figure 11.   RVI Display, RFM, 3-db Threshold

Figure 12. RVI Display, RFM, 6-db Threshold

Figure 13. RVI Display, RFM, 9-db Threshold
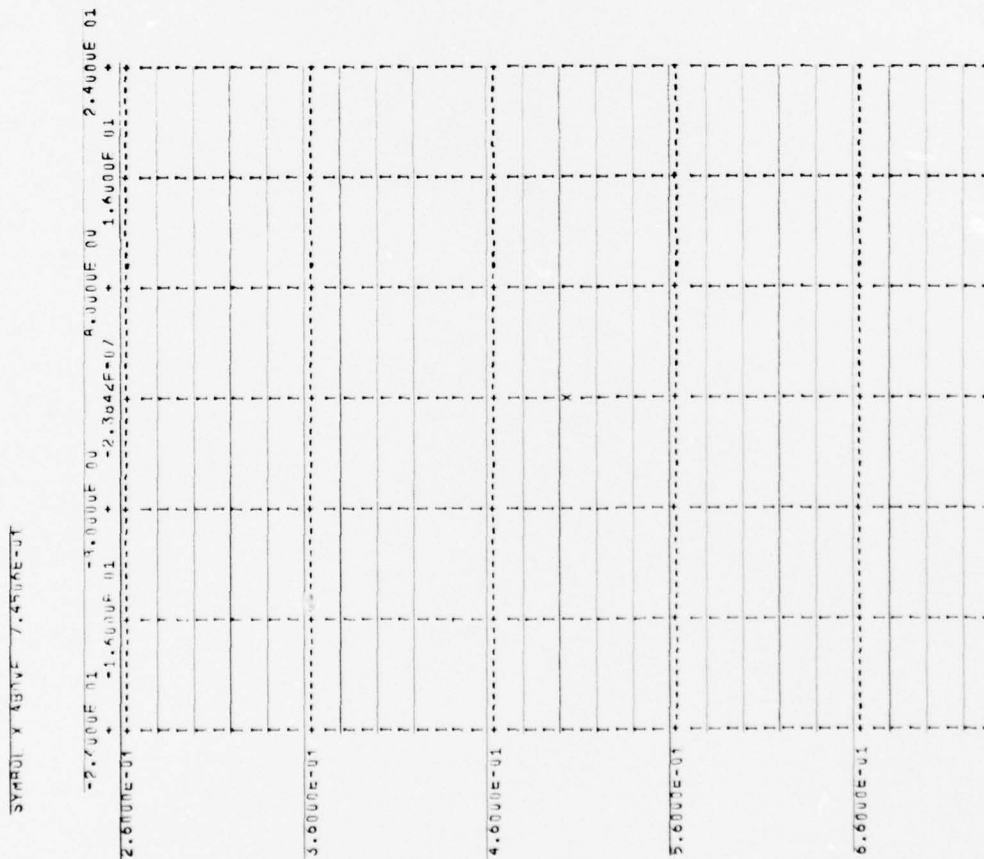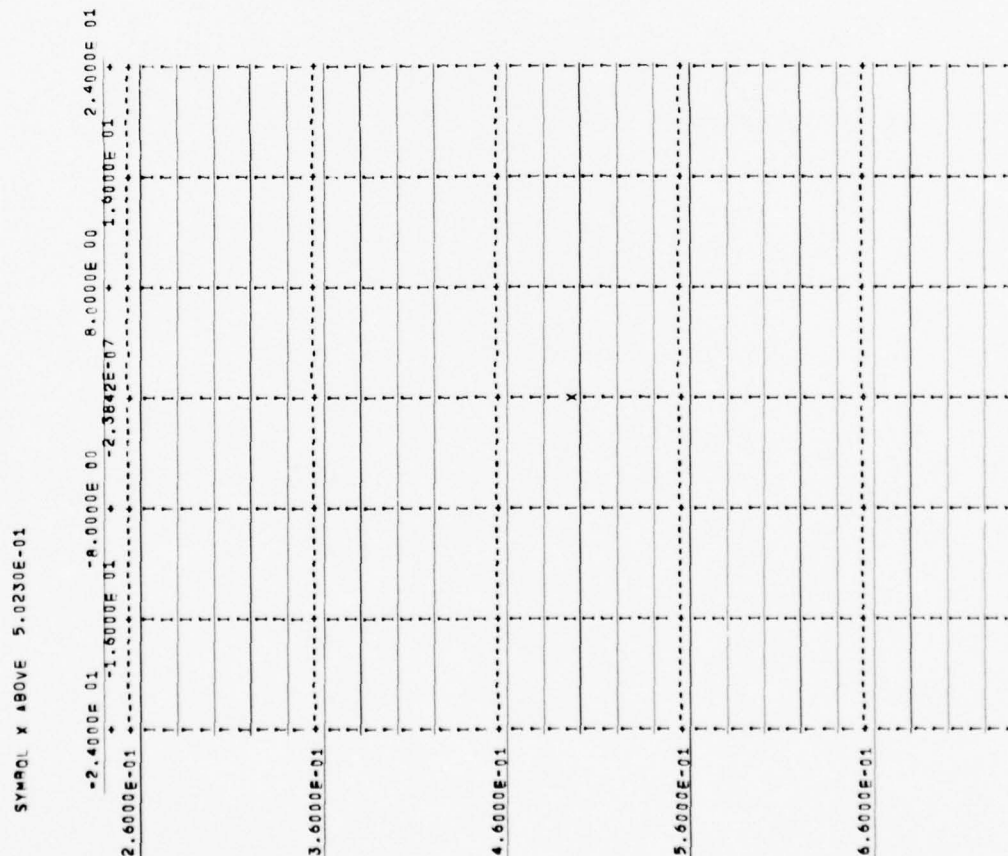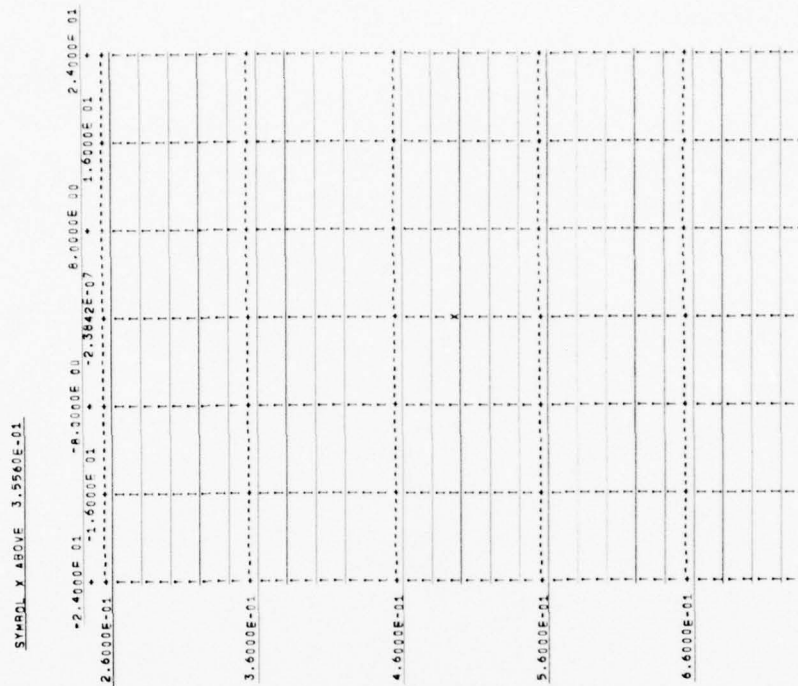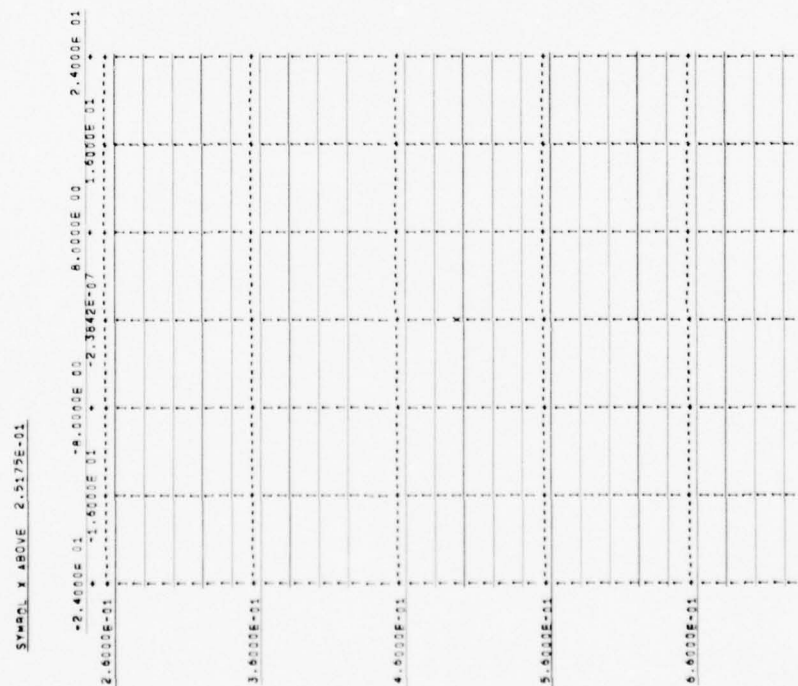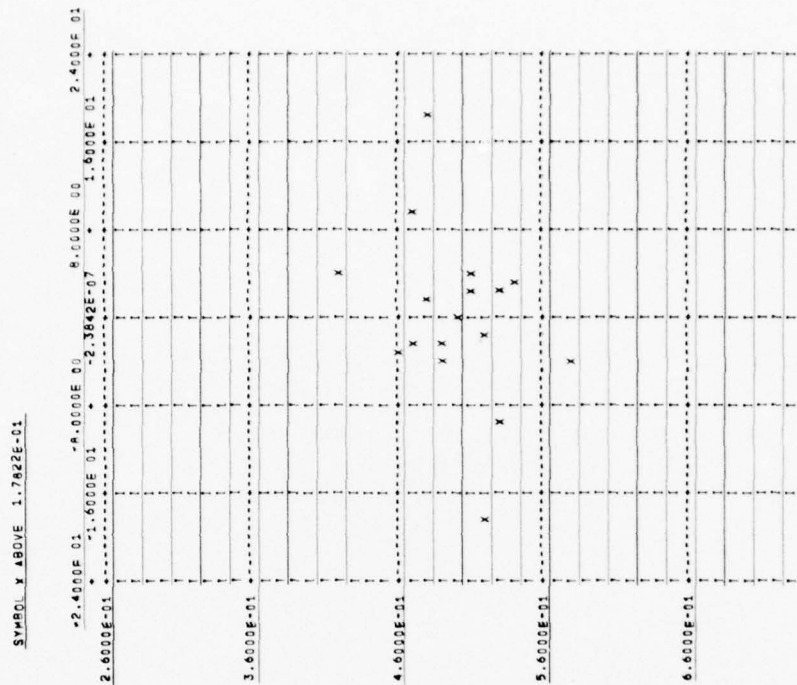
Figure 14. RVI Display, RFM, 12-db Threshold
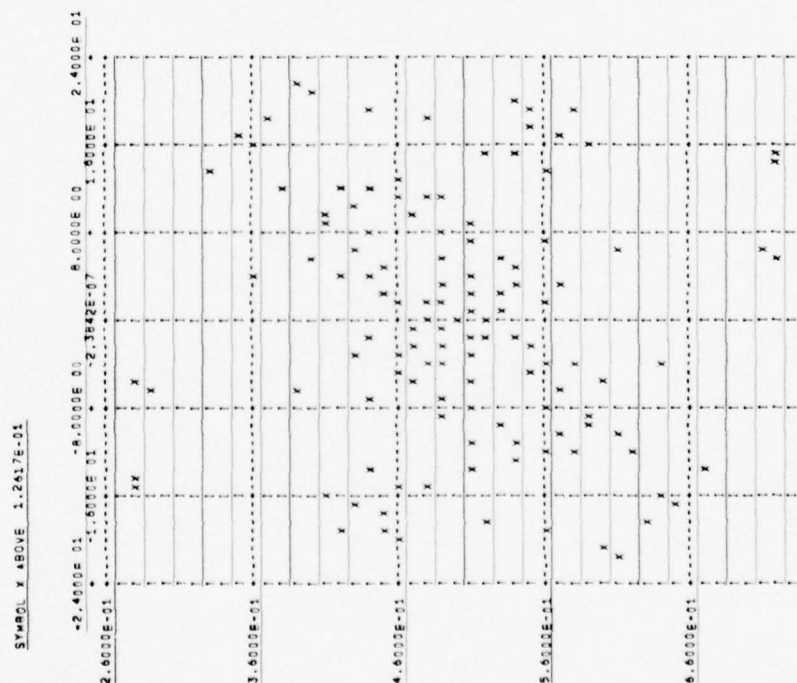
Figure 15. RVI Display, RFM, 15-db Threshold

III. BOTTOM BOUNCE SIMULATION

    A. GENERAL DISCUSSION

       The three types of waveforms which were used in the sea tests were simulated in Section II, and the ambiguity function surfaces of these three waveforms were examined. A comparison of the simulation results with equivalent results obtained from the test returns of the previous report,* indicates very close agreement. There is no reason, in view of the data just presented, to suspect any serious difficulty with the waveforms generated by the actual AN/SQS-26 equipment. Having thus temporarily eliminated serious waveform distortion as a possible explanation for the difficulties encountered in sea-data processing, other possible problem areas must be investigated. Two conceivable environmental effects could explain the disappointing results obtained in the processing of the sea data.* Time spreads or multipath spreads as were evidenced in the sea data represent a medium characteristic which can have serious consequences in the performance of the signal processing system; in addition, time variations of the medium or environment can result in frequency spreading of the received signals and this effect can also contribute to significant performance degradation.

       Since frequency spreading and time spreading of the received signals are present in the actual operating environment of the sonar system,* the possible mechanisms by which these effects are introduced should be considered. At this point many avenues of approach are open -- in fact too many. One can construct mathematical models of the environment and obtain results which will give reasonable answers. For example, if the multipath spreads and/or frequency spreads are assumed to be sufficiently large, serious loss in performance would be indicated by the mathematics. Conversely, if these spreading parameters are assumed to be sufficiently small, then a negligible performance degradation would be predicted by the mathematical results. The obvious answer to this dilemma lies in obtaining appropriate measurements of the sonar environment; unfortunately, there appears to be very little pertinent data of this nature available.

       Faced with this situation, a physical model has been constructed of bottom-bounce transmission, albeit, a model for which no rigorous justification can be presented at this time. The model to be described seems reasonable and the results obtained from this model are not in contradiction with the limited experimental data which has already been gathered.

B. MODEL DESCRIPTION

Let us consider one-way, bottom-bounce transmission from a ship (S) to a target (T) as indicated in Figure 16. If all anomalous effects which may be caused by the water itself are ignored, then the simplest propagation mechanism between ship and target would involve a specular or mirror-like reflection from the bottom as indicated by the solid line from the ship to the bottom and hence to the target. If the dominant mechanism involves specular reflection, then motions of the ship and target relative to the bottom are of no consequence and only the relative motion between ship and target would have to be considered in the analysis. Under such idealized conditions only one ray path would be involved in the transmission of energy from ship to target, there would be no multipath effects, and doppler or frequency spreading effects could be easily calculated from the resulting simple geometry.

The writer would now like to propose a second mechanism to be considered in bottom-bounce propagation -- that of multiple scattering. In this discussion we do not eliminate the specular mode but, instead, we propose that there are at least two modes involved in bottom-bounce propagation: a specular mode and a scattering mode. We further suggest that the scattering mode may, in many cases, be the predominant mode of transmission so that the bulk of received energy at the target arrives via the scattering mode while only a relatively small percentage of the received energy may be attributed to the specular mode.

In crude support of the scattering model which will be shortly described, the reader is asked to observe the RVI displays for ping 13 of the previous report (Figures 143 to 145).* Ping 13 resulted from an FM transmission but the tape data was gated early so that bottom reverberation was recorded. The RVI displays for this reverberation indicate the effects of a collection of discrete reflectors, some having higher effective amplitudes than others. If a transmitted pulse from the ship, upon striking the bottom, reflects significant energy back toward the sound source itself, why should it not be assumed that similar significant energy scattering takes place from the bottom toward the target? Without further apology we shall now describe the bottom-bounce model which was simulated and tested in the work which follows.

AI284
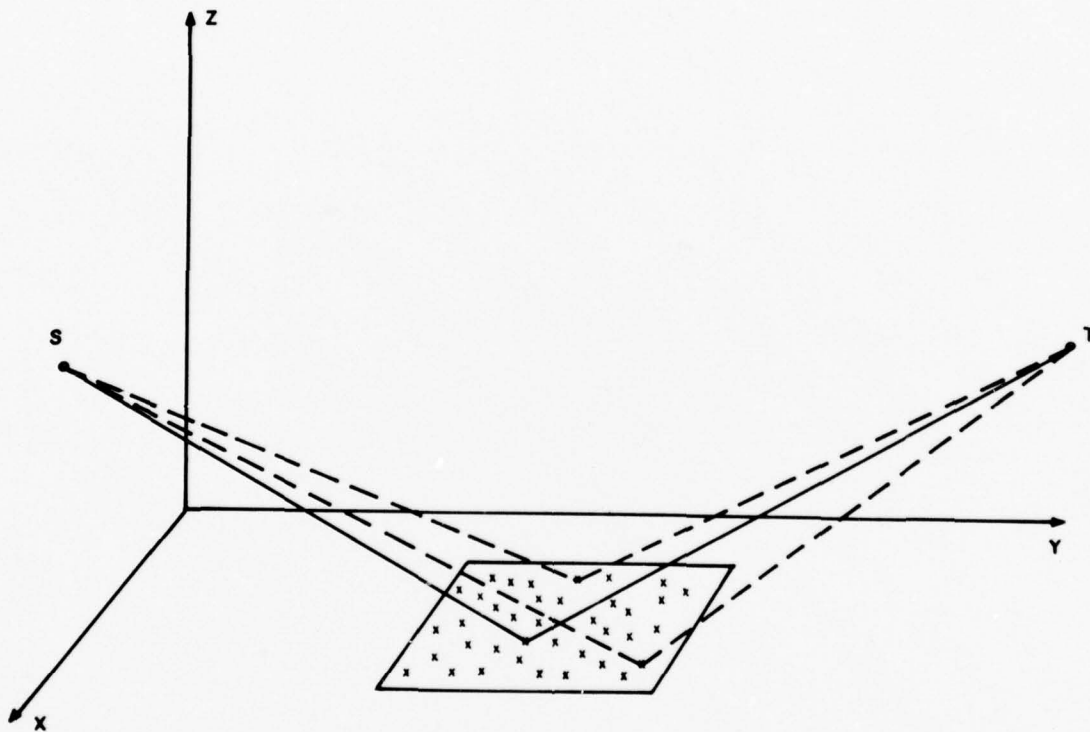

Figure 16. Bottom Bounce Model Geometry

Turning again to Figure 16, it is assumed that the bottom is composed of a large number of discrete scatterers which lie in the area of the bottom illuminated by the array beam. For simplicity, the illuminated area has been assumed to be rectangular having an x dimension determined by the horizontal beam extent measured at beam center on the bottom, and a y dimension determined by the vertical beam extent also measured along beam center on the bottom. Within this rectangle a large number of scatterers or "hot spots" are located randomly. Each scatterer is assumed to contribute to total energy transfer between the ship and the target. In this work the amplitude effects or "transmission factors" of the scatterers are assumed to be uniformly distributed between 0 and 1 and independent from one scatterer to another. A uniform random phase shift (0° to 360°) was also associated with each scatterer, this phase shift being independent from one scatterer to another; thus, energy transmission from the ship (S) to the target (T) of Figure 16 is assumed to take place via a large number of ray paths, two of which are indicated by dashed lines in the figure.

If we suppose that the scattering mechanism just described could represent the dominant mode of energy transmission from ship to target, then some very interesting characteristics of this "transmission path" may be deduced by simple observation. If the ship and target are assumed to be stationary, multipath becomes an obvious consequence of the model. If we imagine short pulses being transmitted from S and received at T, then for each pulse transmitted N pulses will be received, where N represents the number of scatterers being considered. Furthermore, these N received pulses will occur at random times within the multipath spread interval and many of these pulses will overlap in time due to the finite pulse width of the transmission. Thus, if we were to perform an experiment under the conditions just described, we would first of all note that a multipath spread is involved which will be determined by the locations of the ship and target and also by the vertical and horizontal beamwidths of the transmitting array. Since many different scatterers can result in the same or nearly the same one-way path delay, a peak response observed within the multipath spread period at the receiver cannot be attributed necessarily to a single scatterer. Rather, such peak responses are more likely to be caused by a superposition of the energy received via many paths, where chance phasing has resulted in a reenforcement of the total voltage observed at that particular time.

From qualitative considerations as outlined above, we see that the scattering model of Figure 16 results not only in multipath spread or time extent which must be associated with a given transmitted pulse, but that superposition must be considered in explaining the actual amplitude versus time display observed at the target receiver. If the ship is moved from one position to another position relative to the coordinate system of Figure 16, a change in the multipath structure observed at the receiver would be expected. This follows since the superposition effects at the receiver which produce the observed multipath structure will change as the ship position is changed. A chance phasing of scattered pulses which gave reenforcement at a particular time within the multipath structure in the first ship position may result in cancellation in the second ship position. Conversely, such displacement may cause large amplitudes to appear at time positions within the multipath structure where very low amplitudes were formerly noted. Thus it is clear that the "impulse response" of the transmission path from ship to target will be a function, under the assumed model, of ship and target positions. If these positions change with time, then the multipath structure or impulse response of the transmission path must also be expected to change. In fact, as shall shortly be demonstrated, relatively small displacements of ship position can result in rather significant changes in the effective time-domain characteristics of the transmission path from ship to target. This crude model, then, does confirm two effects which have been observed[1] experimentally: a multipath spread in the energy received at the target, and a changing multipath structure from pulse to pulse caused by ship displacement in the interpulse period due to the motion of the ship.

The observed time spreads of received energy and the observed changes in multipath structure from pulse to pulse have been accounted for in the previous discussion. This has been done by a static analysis which argued from the basis of fixed positions for the ship but did not account for ship motion during the transmission period. Frequency and time effects, of course, are closely interrelated, but in the previous discussion the emphasis has been primarily on

---

1 Most observations involve two-way transmission while our discussion is confined to one-way transmission. The extension of one-way effects to the out-and-back case is not too difficult in terms of qualitative descriptions. Such an extension in the quantitative sense is left as an interesting exercise for the reader.

time-domain effects. We now turn our attention to some possible significance that the model of Figure 16 may have relative to the frequency domain.

In investigating frequency-domain effects, the transmission should be changed from a short pulse to a very long (or even a continuous) transmission, and the spectral characteristics of the signal received at the target then observed. If the target is assumed to be stationary while the ship is assumed to have some velocity vector in the coordinate system, the following approximations seem reasonable: the total energy received at the target is represented by a super-position of many signals, each signal component being associated with an individual bottom scatterer; thus, the individual components of the received signal will not only have a random phase and amplitude relative to one another, but there may also exist an actual frequency difference in these various components due to ship motion. It is clear from Figure 16 that if a velocity vector is associated with the ship at point S, this velocity vector will have different component values when projected along the various ray paths from the ship to the bottom scatterers. Thus a multiplicity of doppler frequencies should be in evidence at the target receiver, even though the ship has a unique velocity vector associated with its motion. This is an obvious consequence of the scattering geometry of Figure 16.

In Sections III-C and III-D, the model of Figure 16 is simulated on the computer to form a hypothetical transmission path from ship to target. Short-pulse testing is simulated and time-domain effects are observed in Section III-C; long-pulse testing is done over the simulated channel and spectral analyses or frequency-domain results are observed in Section III-D. The results are interesting and appear to be reasonable.

C.   SHORT-PULSE, TIME RESPONSE TESTS

In this section we consider the time-domain response of the "channel" resulting from the geometry of Figure 16 when short (10 msec) pulses are transmitted from the ship and received at the target. The locations of the 2000 randomly-positioned scatterers involved in this simulation are shown in Figure 17. The ship is placed approximately 2700 fathoms above the bottom and the trans-mitting array is depressed 30°. The vertical beamwidth is assumed to be 21° and the horizontal beamwidth is assumed to be 8.5°. As explained previously, a rectangular area on the bottom is assumed to be illuminated. It is shown in

Figure 17, for the parameters given, that this rectangle has (approximately) an extent of 5000 feet in the x direction and an extent of 27,000 feet in the y direction. The dimensions shown in Figure 17 are in feet and are related to the coordinate system of Figure 16. The scatterers are located in a random (uniform) manner within the rectangle by the computer program. The location of scatterers is shown by the symbol "X" in Figure 17 and there may be (for those who like to count) fewer than 2000 symbols on the page due to the fact that for very-closely spaced scatterers a single X is printed to represent two or more such scatterers. Figure 17 is not particularly significant but it was produced to provide at least a rough check on the performance of the computer program.

A 10-msec pulse is transmitted from the ship; the output of an envelope detector attached to the IF strip of a target receiver is shown in Figures 18 through 22. If a single scatterer were considered, these figures would show a single, square pulse covering six divisions of the x axis. From the headings of Figures 18 through 22; it may be seen that a time spread of 0.2654 second between the longest and shortest possible paths is involved for this particular geometry. The differences which appear in the various plots are caused by four-foot displacements of the ship position along the y axis of the coordinate system of Figure 16; that is, Figure 18 involves no displacement of the ship position from its initial coordinate location, while Figure 19 is the time response observed when a y change in ship position of four feet is introduced. The displacement continues in increments of four feet until a total displacement in the y direction of 16 feet is accrued (Figure 22). It is to be noted that the multipath structure does change from one ship position to another in spite of the fact that relatively small increments in position (four feet) are involved.

Several runs of the type shown were made involving displacements in the other two coordinate directions and the results are very much the same as those shown; therefore, Figures 18 to 22 are presented as being representative of the time-domain effects observed under these conditions of computer simulation. The results, in light of the previous discussion, are not at all unexpected. The changing multipath structure with ship position is clearly evident in the plots and the effects of pulse superposition at the receiver are clearly in evidence; for example, the dominant peak near the beginning of the multipath spread period is obviously not caused by a single transmission path component. If only one

path were involved in this response then a square pulse of six time-unit duration would have resulted as discussed earlier. The fact that this peak response in Figure 22 shows distortion represents ample evidence that superposition effects are responsible for this peak. As further evidence of this phenomenon, compare the time of the peak response of Figure 22 with the response at the same time period in Figure 18. It will be noted that in Figure 18 there is practically a null in this time period, whereas in Figure 22 a rather large response is in evidence; furthermore, a total ship displacement of only 16 feet was involved between Figures 18 and 22.

Little more need be said about the results of Figures 18 through 22 except that care must be taken in interpreting the responses observed. It would appear that a strong path has appeared near the beginning of the multipath spread interval (Figure 22). Actually, this response does not represent one strong path but a superposition of many, much weaker paths, giving the appearance of a strong, single path.

D. LONG-PULSE, FREQUENCY RESPONSE TESTS

In Section III-C, time-response tests were simulated using the scattering model of Figure 16. The results obtained are reasonable and consistent with much of the sea data results. We now turn our attention to the frequency domain which posed a considerable problem in the processing of actual sea data.

A review of the previous report* will reveal that for the two modulation types which provided good doppler resolution (PRN and RFM), extensive spreads were noted in the RVI displays in both time and frequency; in fact, the frequency spreads observed* were often extremely surprising -- the RVI displays showing considerable energy at apparent velocities in the neighborhood of ± 25 knots. The question was raised* (but certainly not answered) as to whether the RVI displays were revealing a true doppler spread of this fantastic extent (true relative doppler was usually zero) or whether other causes might be responsible for the apparent doppler spread of the targets which were observed. An attempt to obtain a partial answer to this question shall be made here.

If the channel model of Figure 16 is assumed to be a reasonable one, then frequency-domain analysis may be carried on by further simulation. Instead of transmitting a short 10-msec pulse as was done in Section III-C, we now

transmit a pulse having a duration of 0.5 second. Such a pulse, of course, has excellent doppler resolution but very poor range resolution -- which is precisely what is desired, since we are now interested in investigating the frequency-domain effects of the assumed model of Figure 16.

In Section III-C only ship displacements were involved in the calculations; no ship velocity was considered. In this section a reverse situation is imposed; that is, ship displacements are ignored but a velocity vector is considered with respect to the ship at point S in Figure 16.

The computer simulation program previously used was modified to provide for a doppler analysis of the received waveform at poing T of Figure 16 when a single pulse of 0.5 second duration was transmitted at S with a ship velocity vector at S being assumed. Even though frequency-domain analysis is to be performed, one must still consider the multipath spread in this case; that is, a single 0.5-second pulse is transmitted but a multiplicity of such pulses are received at point T so that the total duration of the received signal at T will be in excess of the pulse length by an amount equal to the multipath spread. To account for this, the doppler analysis portion of the computer simulation operated in the following manner. The earliest-arriving path time is noted as is the latest-arriving path time. These two times are averaged to give a third time which represents the center of the multipath spread interval. A 0.5-second time gate is then generated by the computer which samples the received signal waveform for doppler processing. Three gating-filtering computations are performed; the first gate starting at the beginning of the multipath spread interval, the second gate starting at the center of the multipath spread interval, and the third gate starting at the end of the multipath spread interval. The outputs of these three gates are processed in a doppler bank containing 61 filters with the center filter (number 31) being set for zero doppler. The bandwidths of these filters are consistent with the 0.5-second transmitted pulse. The results obtained from such spectral analysis processing are shown in Figures 23, 24, and 25.

The header of Figure 23 reveals that the ship and target coordinates are the same as those used in Section III-C. Further, the sonar array parameters are also seen to be the same and, although not explicitly indicated by the header, the bottom-scattering situation is also the same as in the previous section. A ship velocity vector of 10 knots magnitude is assumed with this vector having

equal x and y components of 7.07 knots. The particular doppler bank simulated by the computer in this case uses filters having an effective bandwidth of about 3.4 knots and the center-frequency spacing between these filters is approximately 1.6 knots. By way of added explanation, the computer determines, from the ray-path geometry, both the maximum and minimum doppler shifts. These two items are listed in the header of Figure 23 and it is seen that the maximum doppler was about seven knots while the minimum doppler was about 4.7 knots. This spread arises, of course, due to the varying projections of the ship's velocity vector on the various ray paths from ship to bottom-scattering points.

The plot of Figure 23 shows filter number along the x axis and voltage response (linear detector) along the y axis. The zero doppler filter is numbered 31 and there are 30 filters each side of this one for a total of 61 filters in the bank. As may be seen from Figure 23, the maximum response occurred in filter No. 35 which represents 6.4 knots of one-way doppler. It is further to be noted that the frequency distribution is well confined about this peak.

Figures 24 and 25 are the same as 23, except for the time of the 0.5-second sample of input information as previously explained. There are differences in amplitude in these latter two figures as compared to Figure 23, but the received energy is still seen to be quite well-confined around doppler filters 34 to 36 which is consistent with the maximum and minimum dopplers known to exist. Other similar runs were made using different ship velocities and different scattering distributions, but the results were quite similar to those shown; thus, these results may be taken as representative of this particular type of test.

These frequency-domain results are discouraging in the sense that they do not begin to explain the apparent frequency spreads that were observed in the sea data described in the previous report; thus, the model of Figure 16, while it does predict that a doppler spread of received energy will exist, yields quantitative data (such as that shown in Figures 23 through 25) which do not offer the explanation sought for the frequency spreads "seen" in the actual sea data.

SHIP COORDINATES (FEET)
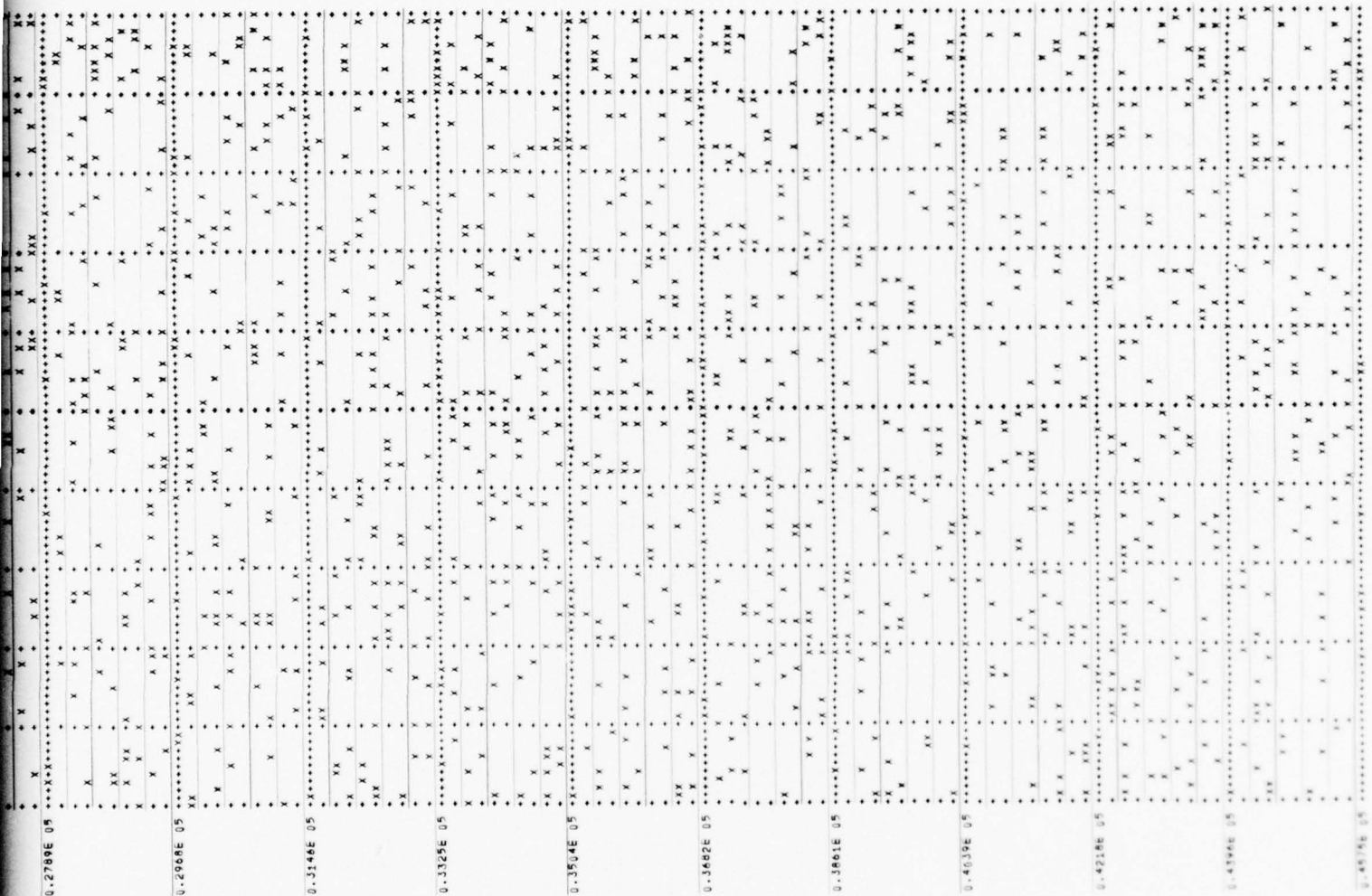X= 0.
Y= 0.
Z= 16200.00

TARGET COORDINATES (FEET)
X= 0.
Y= 04720.00
Z= 16150.00

SHIP DISPLACEMENT (FEET)
X-CHANGE= 0.
Y-CHANGE= 0.
Z-CHANGE= 0.

ARRAY ANGLES (DEGREES)
DEPRESSION= 30.000
VERT. BW= 21.000
HORIZ. BW= 8.500

NO. SCATTERING POINTS= 2400   INITIAL RANDOM NUMBER=102047363735   FINAL RANDOM NUMBER=25021753435

SOUND VEL. (FPS)= 4837.0   CARRIER FREQ. (CPS)= 3400.00   PULSE LENGTH (SEC)= 0.0100

NO. SAMPLES/PULSE= 6   TARGET RANGE (YARDS)= 21573.34   SHORTEST DELAY (SEC)= 14.9710

LONGEST DELAY (SEC)= 15.6764   TIME SPREAD (SEC)= 0.2654   PLOT START (SEC)= 14.9410

PLOT END (SEC)= 15.2060   TIME SCALE= 0.0017 SEC/DIV   DISPLACEMENT INCREMENT (FEET)= 4.080

LOCATION OF SCATTERING POINTS SHOWN IN PLOT BELOW

BOTTOM VALUE   CENTER VALUE   TOP VALUE
-0.240RE 04   -0.   0.240RE 04

Figure 17. Bottom-Scatterer Locations Used in Simulation
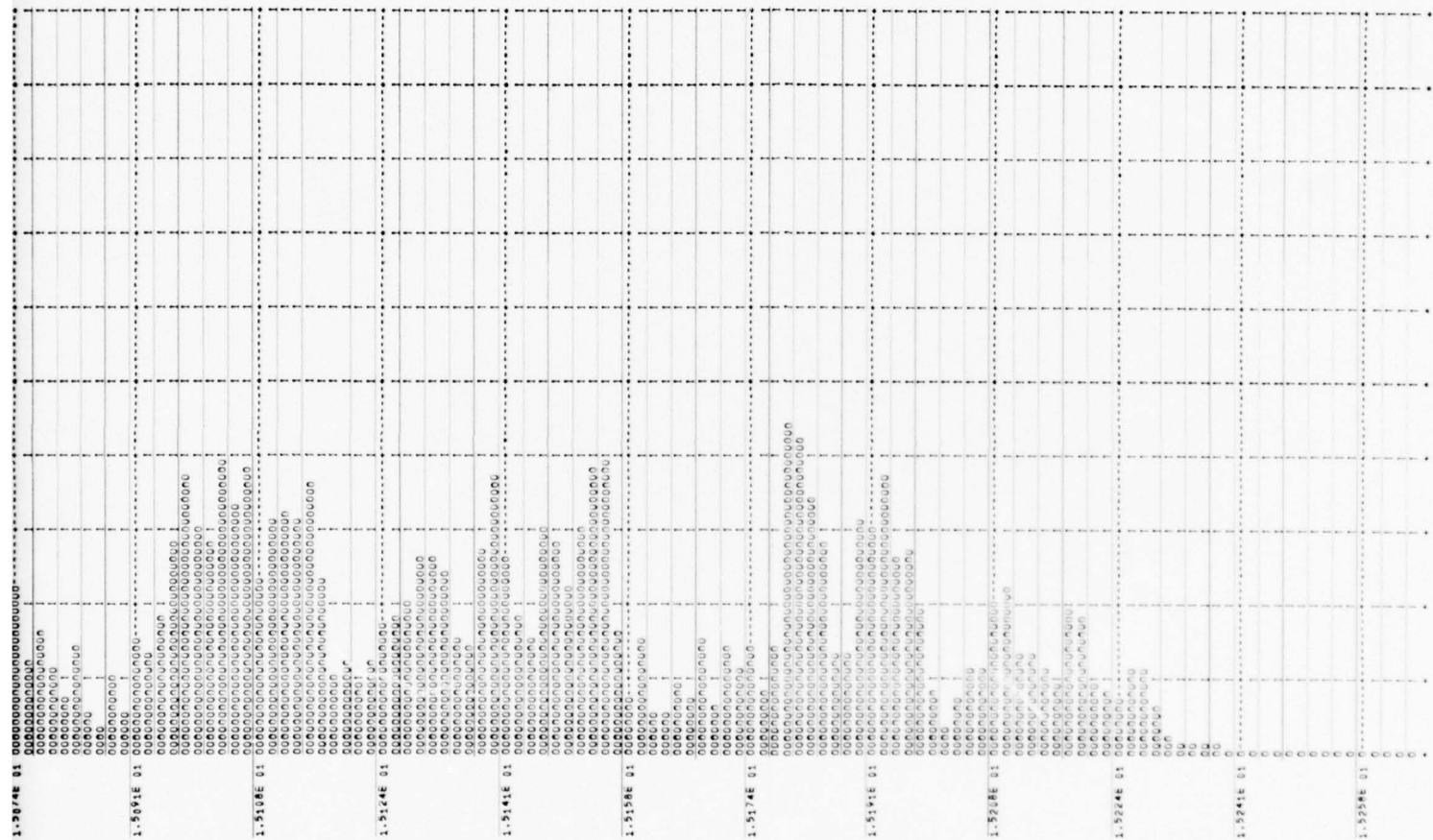
Figure 18.   One-Way Pulse Response via
             Bottom Scatter, Ship Dis-
             placement 0 Feet
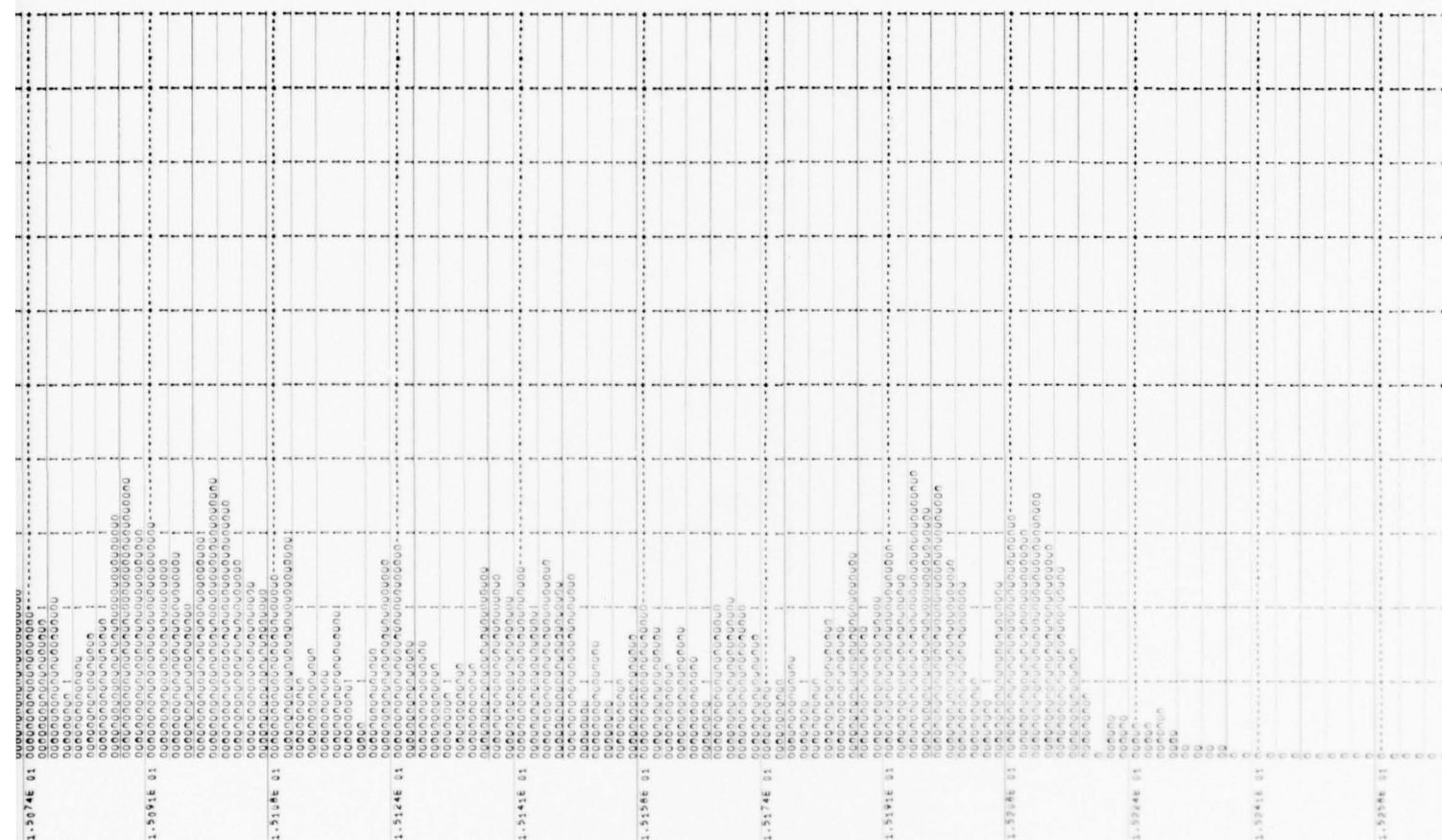
Figure 19. One-Way Pulse Response via
Bottom Scatter, Ship Dis-
placement 4 Feet
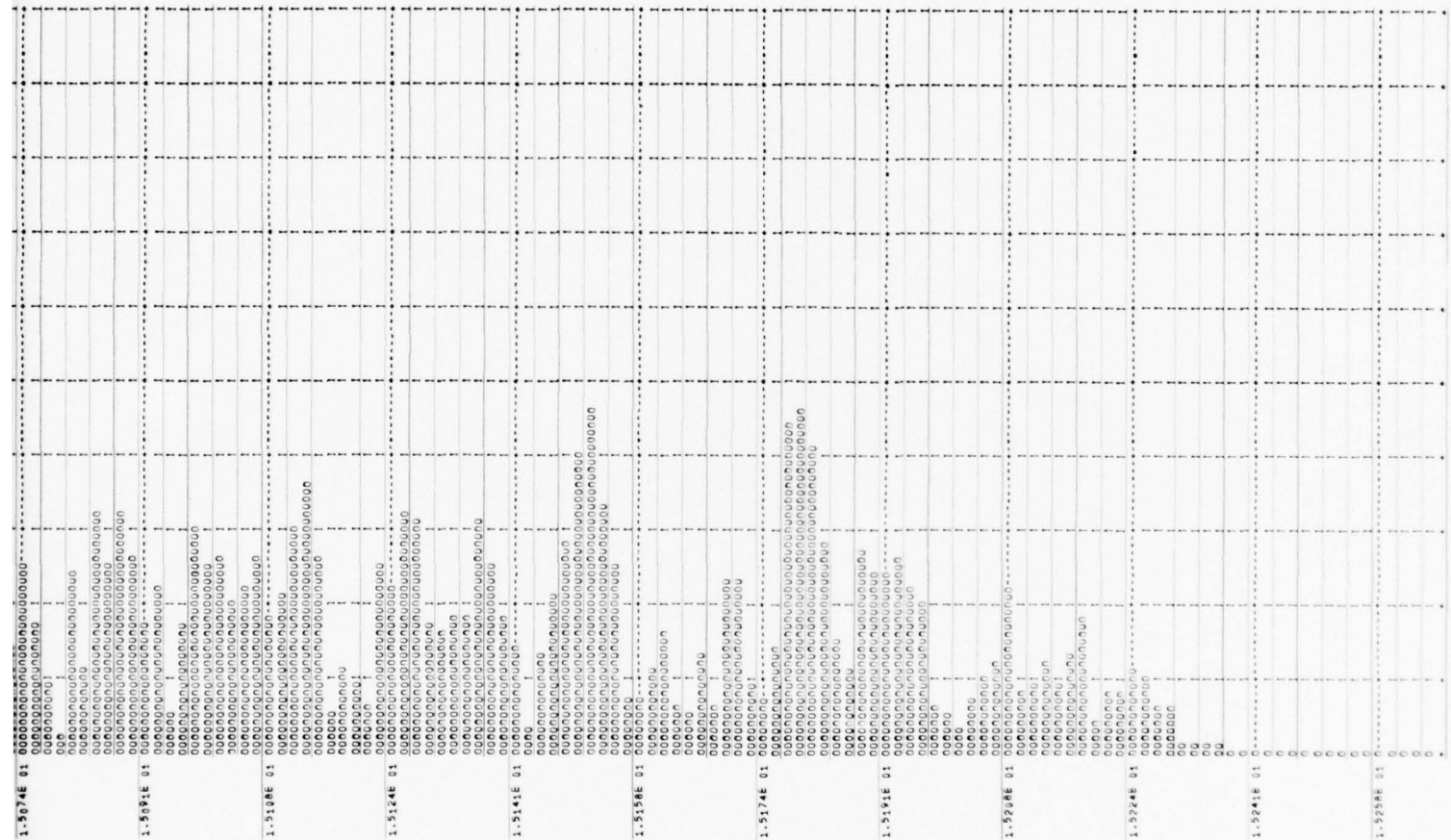
Figure 20. One-Way Pulse Response via
Bottom Scatter, Ship Dis-
placement 8 Feet

28
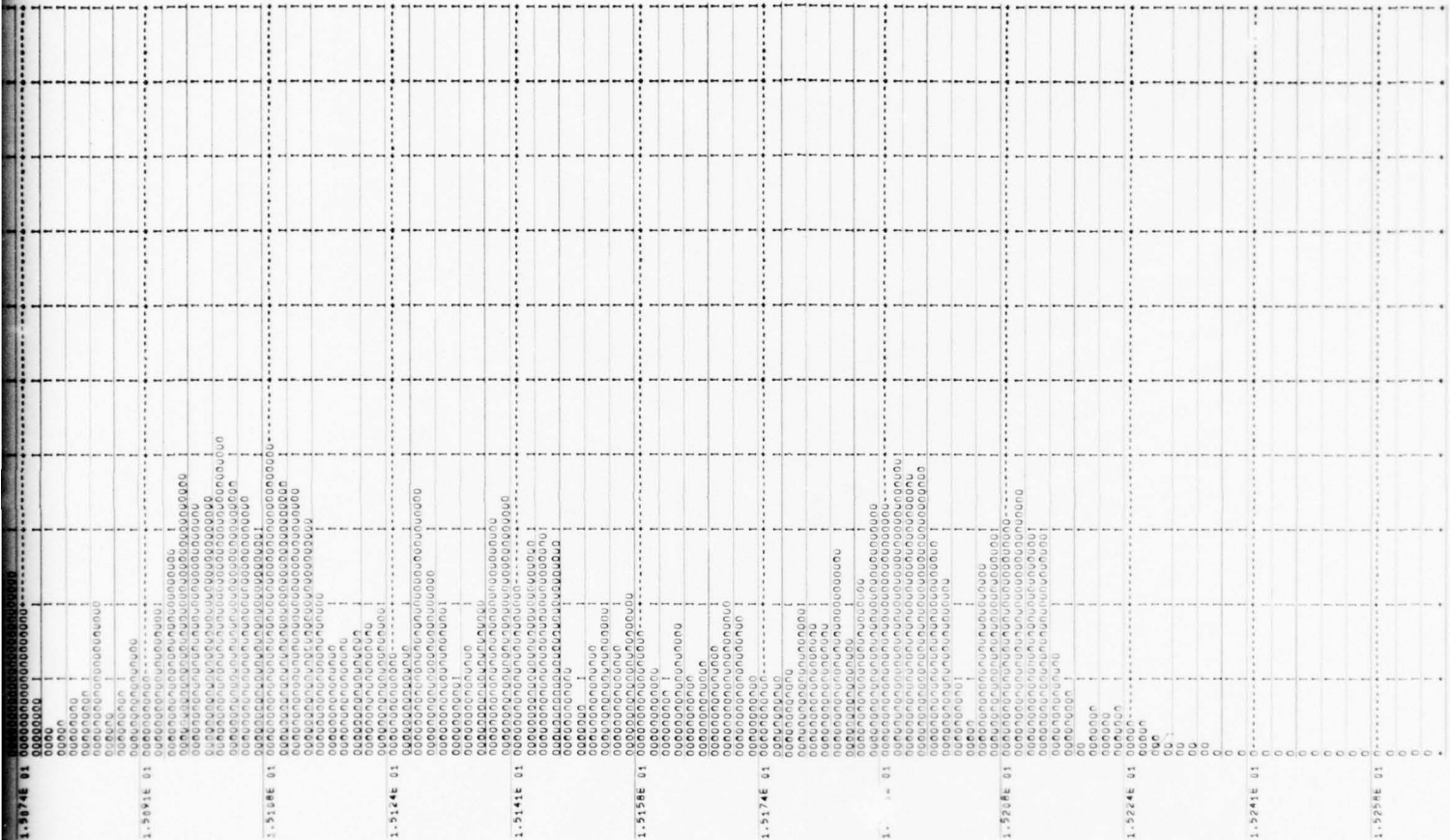
Figure 21.   One-Way Pulse Response via
             Bottom Scatter, Ship Dis-
             placement 12 Feet

29
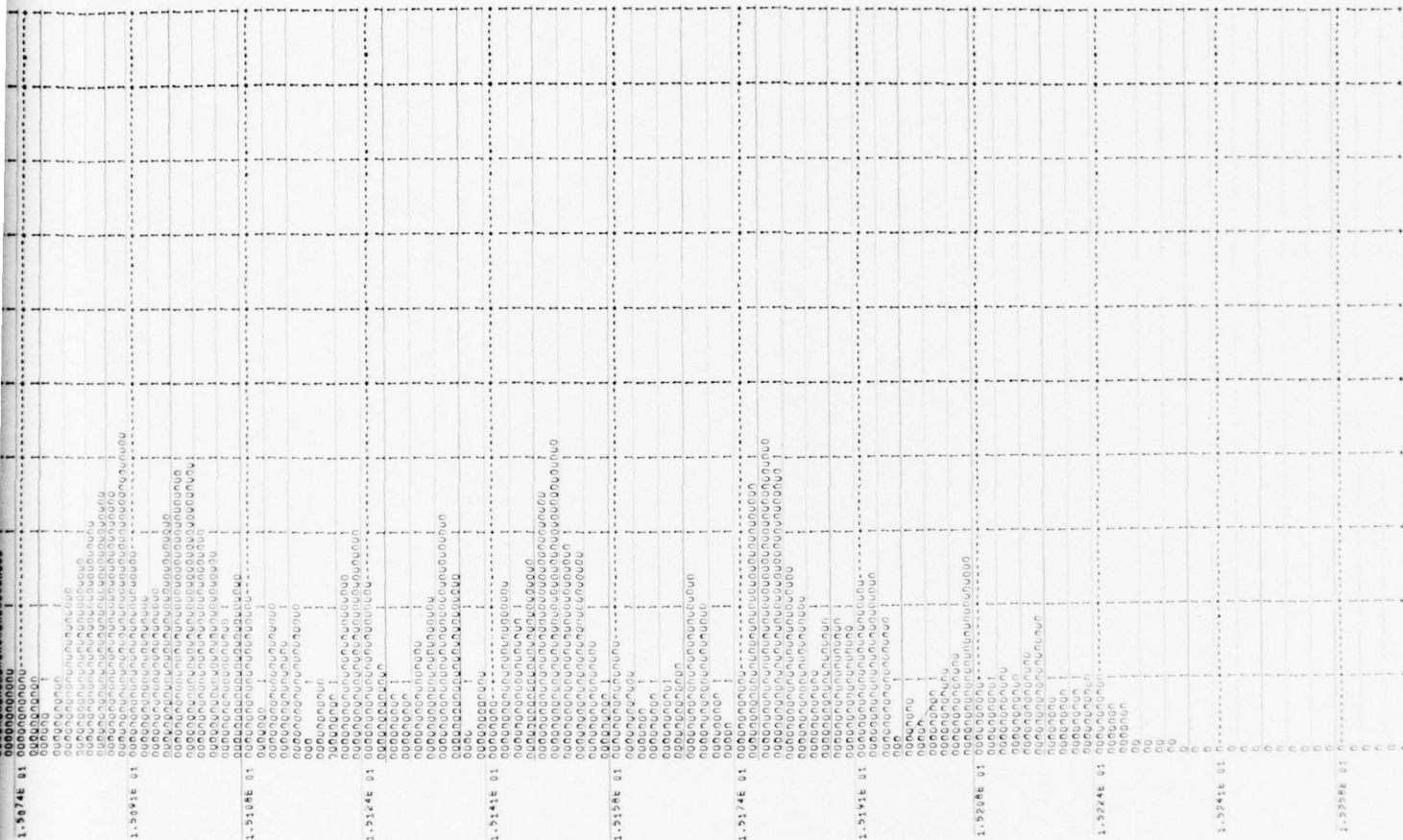
Figure 22. One-Way Pulse Response via
Bottom Scatter, Ship Dis-
placement 16 Feet

SHIP COORDINATES (FEET)	TARGET COORDINATES (FEET)	SHIP VELOCITY (KNOTS)	ARRAY ANGLES (DEGREES)		
X= 0.	X= 0.	X-COMP.= 7.070000	DEPRESSION =	30.000000
Y= 0.	Y=64720.000000	Y-COMP.= 7.070000	VERT. BW. =	21.000000
Z=16200.000000	Z=16150.000000	Z-COMP.= 0.	HORIZ. BW. =	6.500000

|			
SCATTERING POINTS= 2000	SOUND VEL. (FPS) = 4833.000000	PULSE LENGTH SEC = 0.500000
INITIAL RANDOM NO=102047363735	CARRIER FREQ CPS = 3400.000000	SHORTEST PATH SEC= 14.970968
FINAL RANDOM NO. =250217653435	IF FREQUENCY CPS = 100.000000	LONGEST PATH SEC = 15.236371
TARGET RANGE YDS.=21573.339600	SHIP VEL. (KNOTS)= 9.998490	MULT. SPREAD SEC = 0.265403
DOPPLER INC. KTS.= 1.600000	NO. DOP. FILTERS = 61	SAMP. PERIOD SEC = 0.001000
FILTER BW. KNOTS = 3.411529	MAX. DOPPLER KTS = 6.993963	MIN. DOPPLER KTS = 4.673056
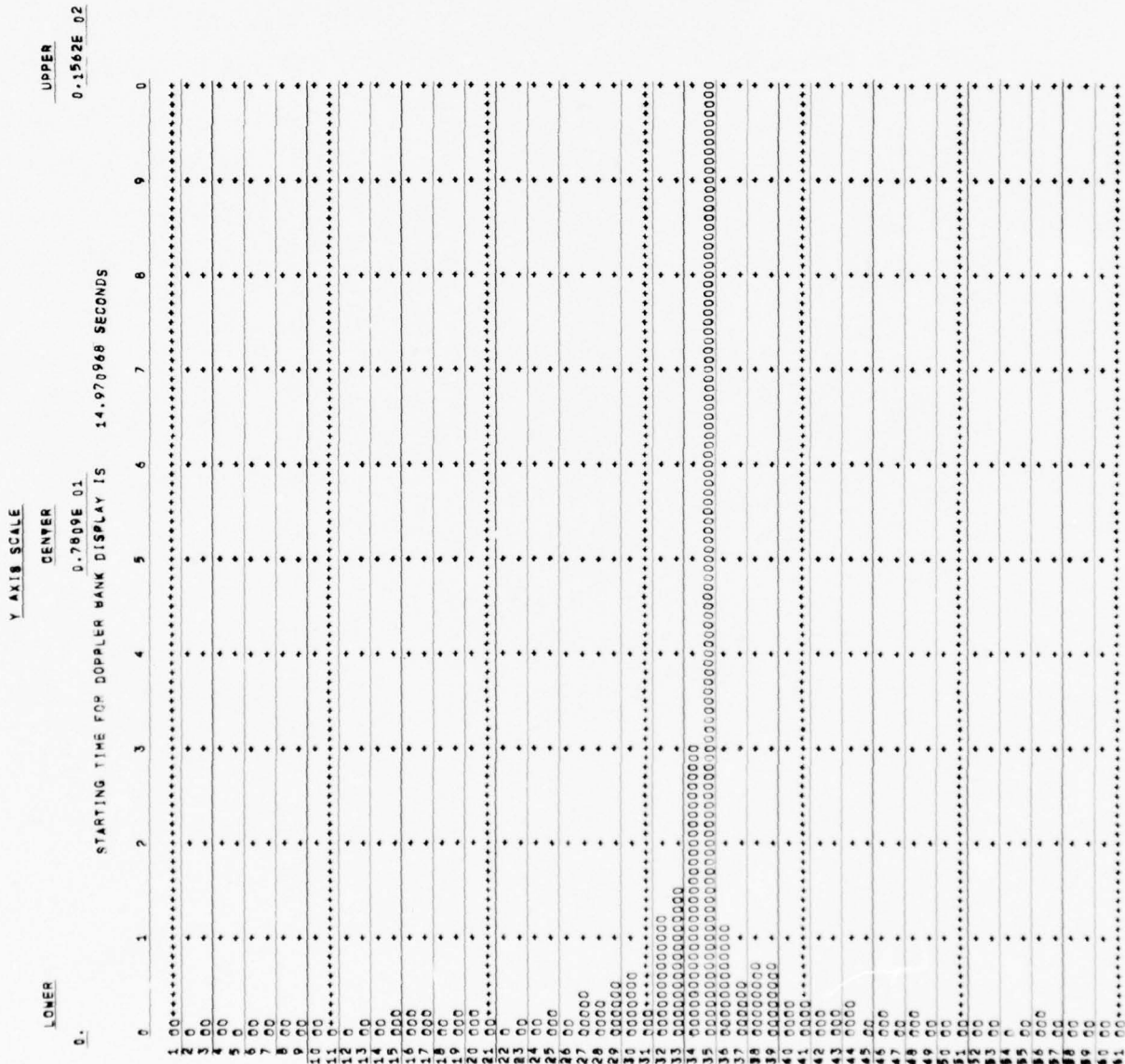
Figure 23. Doppler Analysis, One-Way Pulse Response, First Gate
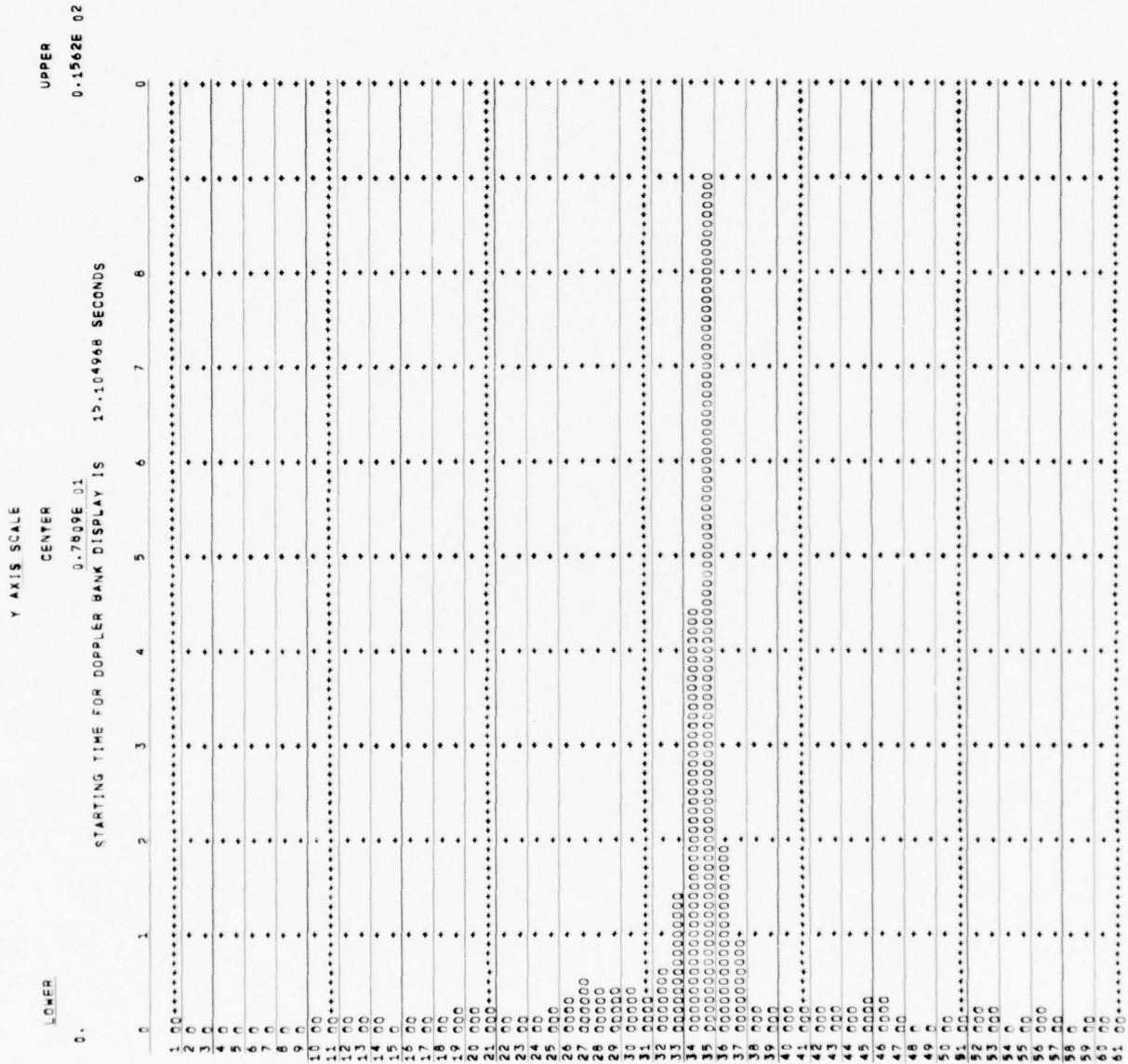
Figure 24. Doppler Analysis, One-Way Pulse Response, Second Gate
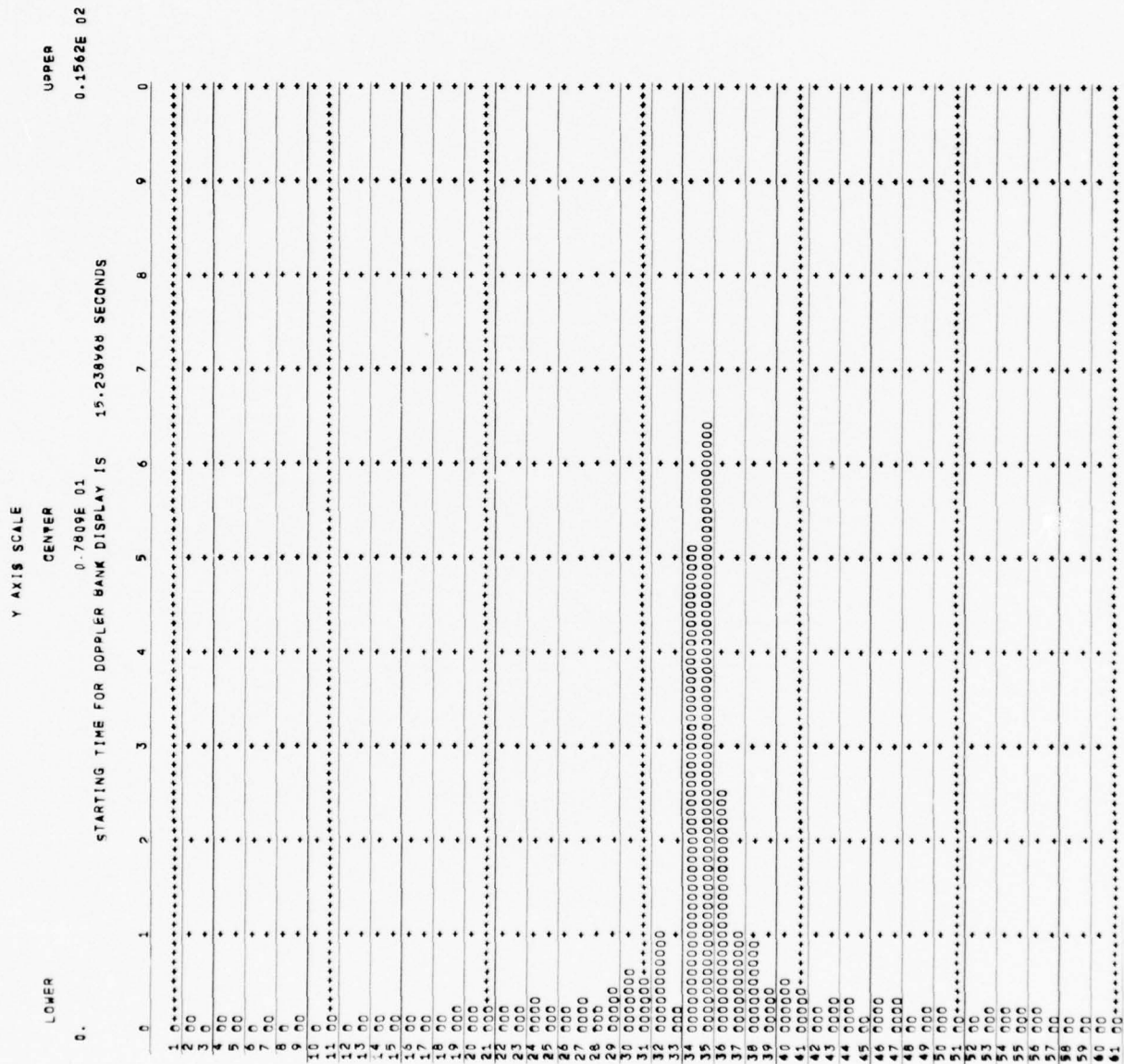
Figure 25. Doppler Analysis, One-Way Pulse Response, Third Gate

IV. SYSTEM PERFORMANCE UNDER SIMPLE MULTIPATH CONDITIONS

If the model of Figure 16 and the corresponding results of Section III are accepted, the time-domain effects observed* can be explained; however, the frequency-domain effects observed* are orders of magnitude greater than would be predicted on the basis of Section III of this report. Certainly, decorrelation effects due to ship and target motion would tend to degrade the performance of coherent processors, and could result in the apparent confusion seen on the majority of the RVI displays* with regard to PRN and RFM pings; however, decorrelation effects shall be ignored here, and only multipath effects will be considered. In other words, the model of Figure 16 will be used, but both the ship and target shall be held stationary -- resulting in multipath effects only. If such conditions are assumed, there is no decorrelation of the signals received via the individual paths; that is, a multiplicity of signals will be received, but each signal received will be a perfect replica of the waveform which was transmitted. Using such a static model for bottom-bounce transmission, the RVI displays which result when the three different types of modulation are employed will be examined to see if multipath alone might represent a plausible explanation for the doppler-spreading effects seen in the RVI displays.*

The time-domain response of Figure 22 was examined and, quite arbitrarily, 16 apparent "paths" were selected. The selection was based upon the peak responses seen, even though some of these "peaks" are quite small. The relative time of arrival of each of the 16 paths was noted, as was the power level of each particular path. These power levels ranged from a peak of unity down to a value of 0.01; thus, the path structure chosen involves a 20-db spread in relative level. With this assumed path structure, a system simulation was then run using an "ideal" processor which produced RVI displays equivalent to those shown in the previous report. Three modulation types were tested: FM, PRN and RFM. In the work which follows no noise was introduced in the simulation process; that is, the multipath situation alone exists at the receiver with no background noise added to the received signal.

The results for FM modulation are shown in Figures 26 through 30. The header in these figures shows the relative time of occurrence of each path and the relative power level of the path, for a total of 16 paths in all. Since a static situation was assumed in the model, no doppler is involved and all returns are

at zero knot. Figures 26 through 30 are quite consistent with what was seen in the sea data for this type of modulation. At the higher threshold settings only the ridges from the stronger paths are seen; as the threshold setting is progressively lowered, additional ridges come into evidence. As is characteristic of FM, the low threshold setting of 15 db of Figure 30 leaves considerable "white space" on the display, indicating that the volume under the ambiguity surface for this type of modulation is well-confined to the region of the main ridge. The results shown in these figures agree quite closely with the results of the previous report for pings 17, 319, 323, and 387.

The same results when PRN modulation is employed are shown in Figures 31 through 35. At the 3-db threshold setting (Figure 31) the RVI display reveals two responses at the times which correspond to the two strongest paths of the 16 paths involved. These peak responses occur at zero doppler, which is the correct value in this case. As the threshold is lowered (Figures 32 through 35) immediate trouble is to be seen; for example, in Figure 32 the threshold is set 6 db below the local peak yet "targets" appear with apparent velocities that are quite far-removed from the true velocity of 0 knot. (No noise is present in this simulation; only the 16 multipath returns are being processed.) As the threshold setting is further lowered, a complete "flooding" of the RVI display is to be seen; at the 15 db setting shown in Figure 35, the RVI display is almost completely full. Comment on this effect shall be withheld until the RFM modulation results are examined.

The performance using RFM modulation is shown in Figures 36 through 40, with results that are nearly identical to those obtained using PRN modulation. When the threshold is set near the peak value (Figure 36), reasonable results are obtained; however, as the threshold is lowered (Figure 37), the "flooding" effect again appears in the RVI display. Energy is indicated (Figure 37) at an apparent doppler of almost 16 knots opening and more than 8 knots closing when it is known that every component of the received signal is a perfect replica of the transmitted signal and has zero doppler. As the threshold is lowered, the RVI displays rapidly "flood" until, at the 15-db level (Figure 40), the display is almost completely full.

Figures 31 through 40 are quite interesting since they show results which are typical of those obtained* using actual sea data. It is also to be noted

that these results are obtained from simple multipath assumptions; no decorrelation or noise effects are involved in the simulation.

SYSTEM PARAMETERS

SYSTEM BANDWIDTH (CPS)	150.000000
SIGNAL BANDWIDTH (CPS)	100.000000
CARRIER FREQUENCY (CPS)	3400.000000
DOPPLER FILTER SETTING (KTS)	0.
INITIAL TIME SEARCH (SEC)	0.260000
FINAL TIME SEARCH (SEC)	0.740000
INITIAL TIME SEARCH INDEX	261
FINAL TIME SEARCH INDEX	741
TIME INCREMENT (SEC)	0.001000
SAMPLING RATIO	6.666667
PROPAGATION VELOCITY (KTS)	2900.000000
WAVEFORM TYPE	1
PULSE LENGTH (SEC)	0.500000

NOISE PARAMETERS

INITIAL RANDOM NUMBER	106721074235
FINAL RANDOM NUMBER	106721074235
NUMBER NOISE TERMS USED	265
NUMBER NOISE SAMPLES USED	1503
AVERAGE POWER CALCULATED	0.

REFERENCE PARAMETERS

NUMBER SAMPLE POINTS	501
INITIAL RANDOM NUMBER	123331725215
FINAL RANDOM NUMBER	123331725215
NUMBER NOISE TERMS USED	90

SIGNAL PARAMETERS

NO. TARGETS USED= 16   REFERENCE TARGET POWER= 0.10020E 01

TARGET	TIME	INDEX	POWER
1	0.3700	371	0.5000
2	0.3870	388	1.0000
3	0.4040	405	0.1600
4	0.4130	414	0.3600
5	0.4270	428	0.0900
6	0.4440	445	0.1500
7	0.4600	461	0.2500
8	0.4790	480	0.1600
9	0.4930	494	0.1600
10	0.5050	506	0.0900
11	0.5170	518	0.0900
12	0.5320	533	0.2000
13	0.5630	563	0.1800
14	0.5770	578	0.0630
15	0.5910	592	0.0900
16	0.6080	609	0.0100

(ALL RETURNS AT   0.   KNOTS)

RANGE-VELOCITY DISPLAY DATA

SAMPLING RATE   1000.00/SEC   DISPLAY INDEX   10   PEAK VOLTAGE   0.79767E 0n   DOP. OF PEAK   -4.000 KTS
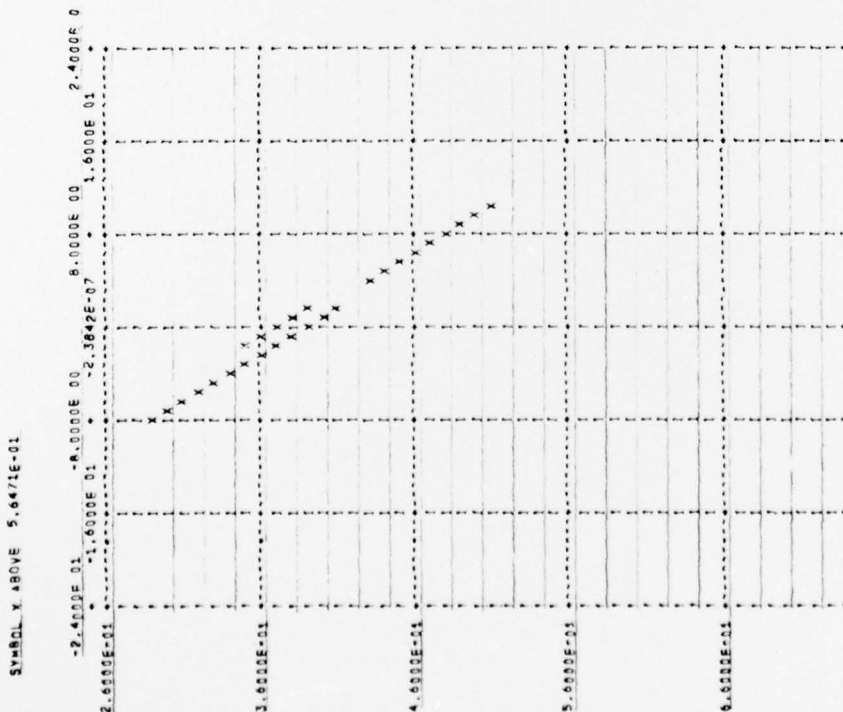TIME OF PEAK   0.34000E-00 SEC   THRESHOLD SETTING   3.00 DB BELOW PEAK

Figure 26.   FM Pulse with Multipath, RVI Display, 3-db Threshold

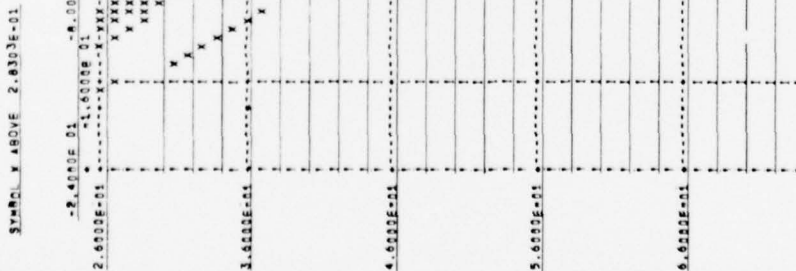Figure 27. FM Pulse with Multipath, RVI Display, 6-db Threshold

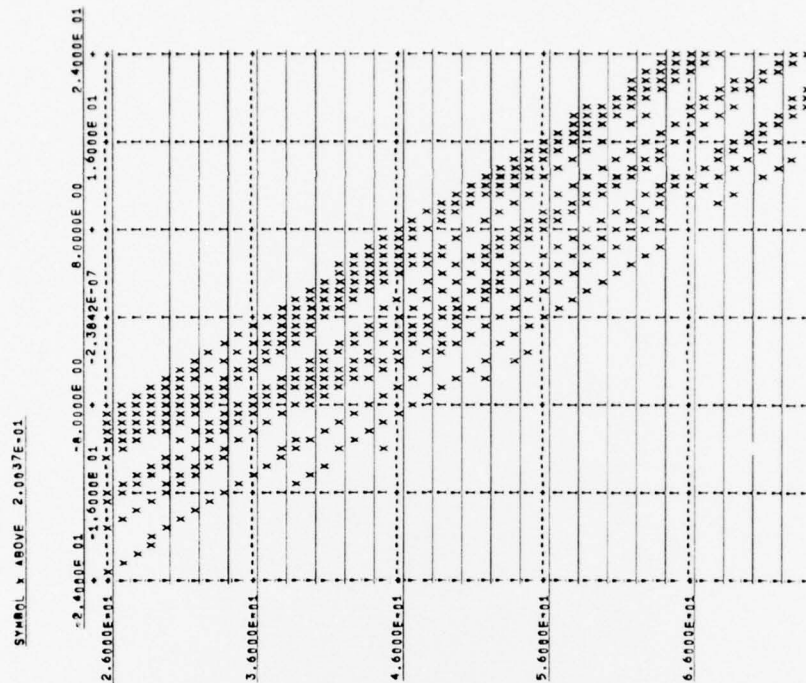

Figure 28. FM Pulse with Multipath, RVI Display, 9-db Threshold

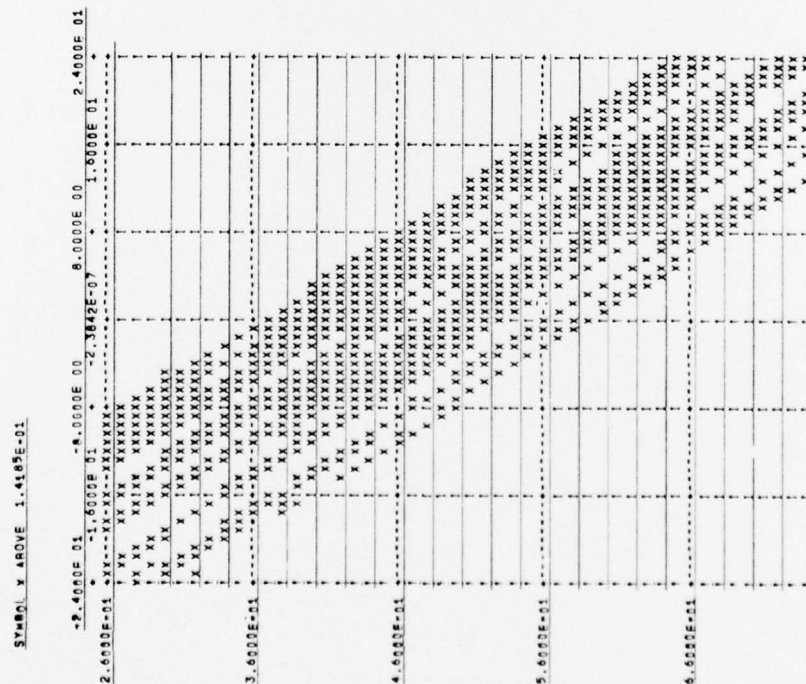Figure 29.   FM Pulse with Multipath, RVI Display, 12-db Threshold

Figure 30.   FM Pulse with Multipath, RVI Display, 15-db Threshold

SYSTEM PARAMETERS

SYSTEM BANDWIDTH (CPS)	150.000000
SIGNAL BANDWIDTH (CPS)	100.000000
CARRIER FREQUENCY (CPS)	3400.000000
DOPPLER FILTER SETTING (KTS)	0.
INITIAL TIME SEARCH (SEC)	0.260000
FINAL TIME SEARCH (SEC)	0.740000
INITIAL TIME SEARCH INDEX	261
FINAL TIME SEARCH INDEX	741
TIME INCREMENT (SEC)	0.001000
SAMPLING RATIO	6.666667
PROPAGATION VELOCITY (KTS)	2900.000000
WAVEFORM TYPE	3
PULSE LENGTH (SEC)	0.500000

NOISE PARAMETERS

INITIAL RANDOM NUMBER	106721074235
FINAL RANDOM NUMBER	106721074235
NUMBER NOISE TERMS USED	265
NUMBER NOISE SAMPLES USED	1503
AVERAGE POWER CALCULATED	0.

REFERENCE PARAMETERS

NUMBER SAMPLE POINTS	501
INITIAL RANDOM NUMBER	123331725215
FINAL RANDOM NUMBER	005701402765
NUMBER NOISE TERMS USED	90

SIGNAL PARAMETERS

NO. TARGETS USED= 16   REFERENCE TARGET POWER= 0.10499E 01

TARGET	TIME	INDEX	POWER
1	0.3700	371	0.5000
2	0.3870	388	1.0000
3	0.4040	405	0.1600
4	0.4130	414	0.3600
5	0.4270	428	0.0900
6	0.4440	445	0.1500
7	0.4600	461	0.2500
8	0.4790	480	0.1600
9	0.4930	494	0.1600
10	0.5050	506	0.0900
11	0.5170	518	0.0900
12	0.5320	533	0.2000
13	0.5630	563	0.1800
14	0.5770	578	0.0630
15	0.5910	592	0.0900
16	0.6080	609	0.0100

(ALL RETURNS AT   0.   KNOTS)

RANGE-VELOCITY DISPLAY DATA

SAMPLING RATE 1000.00/SEC   DISPLAY INDEX   10   PEAK VOLTAGE 0.10613E 01   DOP. OF PEAK -0.000 KTS
TIME OF PEAK 0.39000E-00 SEC   THRESHOLD SETTING   3.00 DB BELOW PEAK
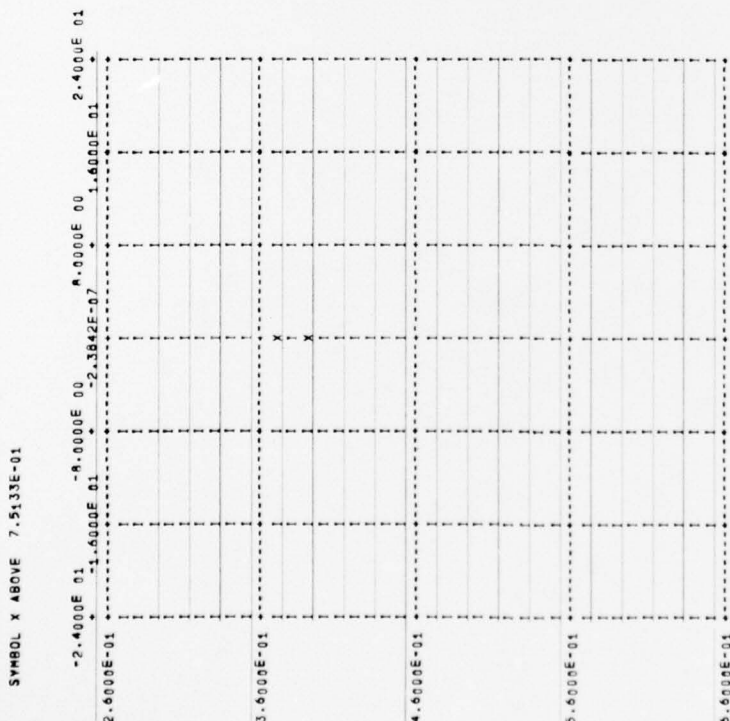

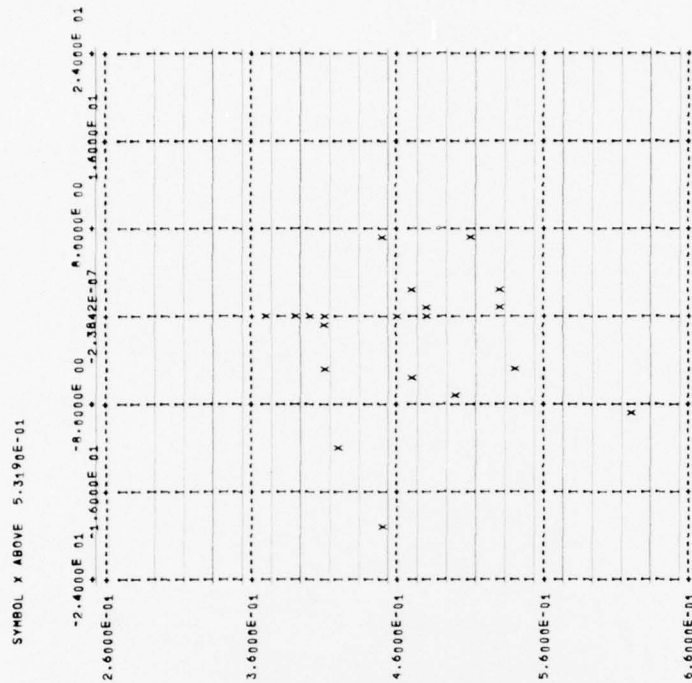
Figure 31.   PRN Pulse with Multipath, RVI Display, 3-db Threshold

Figure 32.   PRN Pulse with Multipath, RVI Display, 6-db Threshold

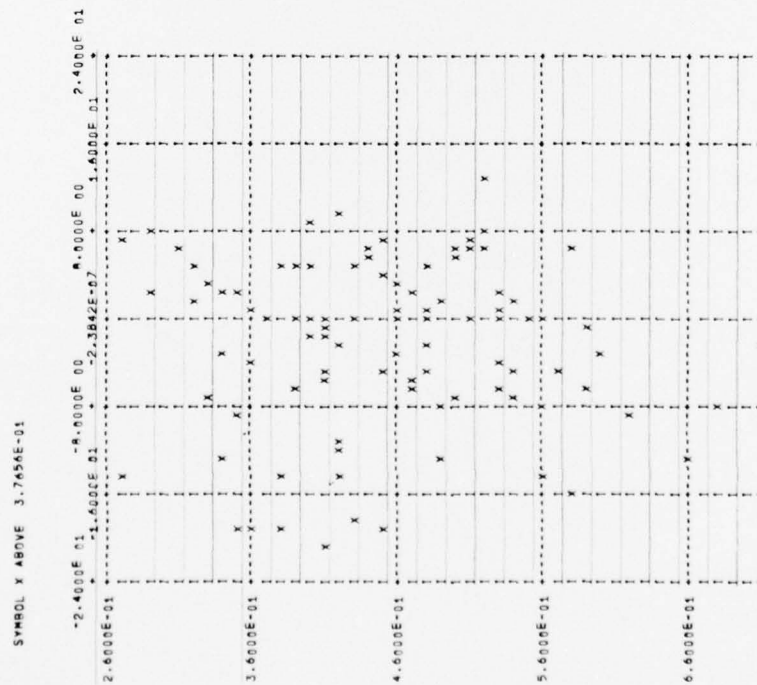
Figure 33.   PRN Pulse with Multipath, RVI Display, 9-db Threshold
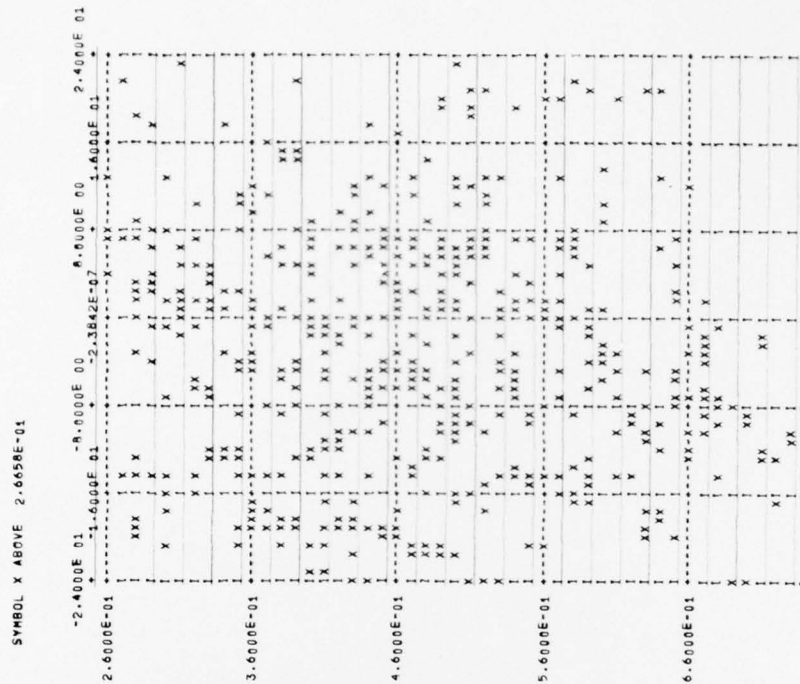
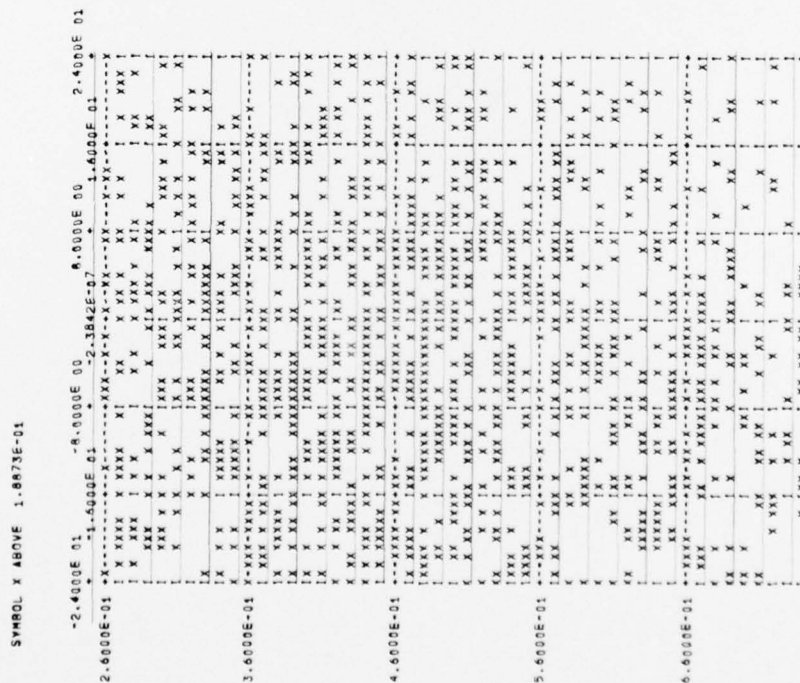Figure 34. PRN Pulse with Multipath, RVI Display, 12-db Threshold

Figure 35. PRN Pulse with Multipath, RVI Display, 15-db Threshold

SYSTEM PARAMETERS

SYSTEM BANDWIDTH (CPS)	150.000000
SIGNAL BANDWIDTH (CPS)	190.000000
CARRIER FREQUENCY (CPS)	3400.000000
DOPPLER FILTER SETTING (KTS)	0.
INITIAL TIME SEARCH (SEC)	0.260000
FINAL TIME SEARCH (SEC)	0.740000
INITIAL TIME SEARCH INDEX	261
FINAL TIME SEARCH INDEX	741
TIME INCREMENT (SEC)	0.001000
SAMPLING RATIO	6.666667
PROPAGATION VELOCITY (KTS)	2900.000000
WAVEFORM TYPE	4
PULSE LENGTH (SEC)	0.500000

NOISE PARAMETERS

INITIAL RANDOM NUMBER	106721074235
FINAL RANDOM NUMBER	106721074235
NUMBER NOISE TERMS USED	265
NUMBER NOISE SAMPLES USED	1503
AVERAGE POWER CALCULATED	0.

REFERENCE PARAMETERS

NUMBER SAMPLE POINTS	501
INITIAL RANDOM NUMBER	123331725215
FINAL RANDOM NUMBER	123331725215
NUMBER NOISE TERMS USED	90

SIGNAL PARAMETERS

NO. TARGETS USED= 16   REFERENCE TARGET POWER= 0.99989E 00

TARGET	TIME	INDEX	POWER
1	0.3700	371	0.5000
2	0.3870	388	1.0000
3	0.4040	405	0.1600
4	0.4130	414	0.3600
5	0.4270	428	0.0900
6	0.4440	445	0.1500
7	0.4600	461	0.2500
8	0.4790	480	0.1600
9	0.4930	494	0.1600
10	0.5050	506	0.0900
11	0.5170	518	0.0900
12	0.5320	533	0.2000
13	0.5630	563	0.1800
14	0.5770	578	0.0630
15	0.5910	592	0.0900
16	0.6080	609	0.0100

(ALL RETURNS AT   0.   KNOTS)

RANGE-VELOCITY DISPLAY DATA

SAMPLING RATE   1000.00/SEC   DISPLAY INDEX   10   PEAK VOLTAGE   0.63180E 00   DOP. OF PEAK -0.000 KTS
TIME OF PEAK 0.39000E-00 SEC   THRESHOLD SETTING   3.00 DB BELOW PEAK
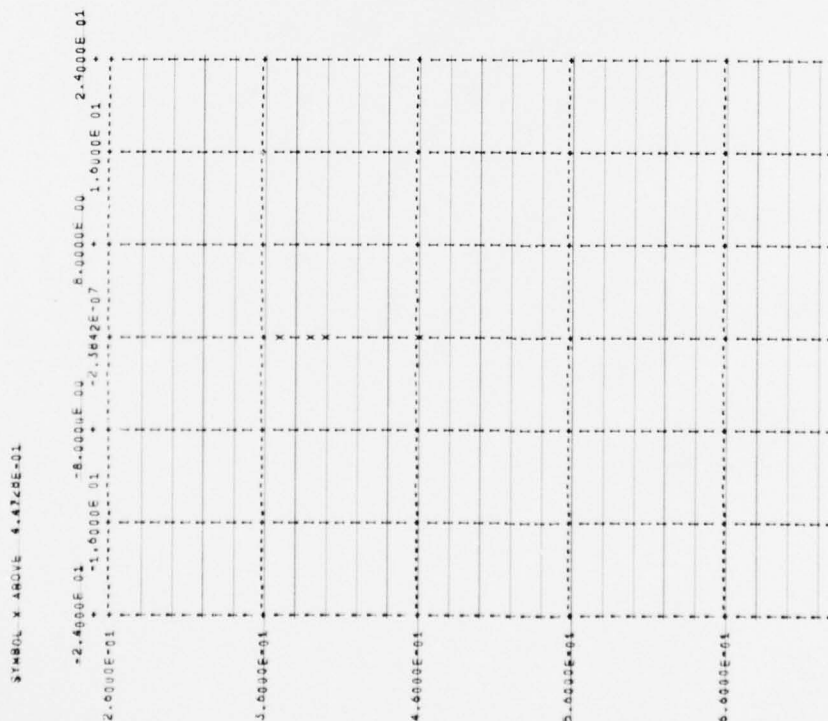

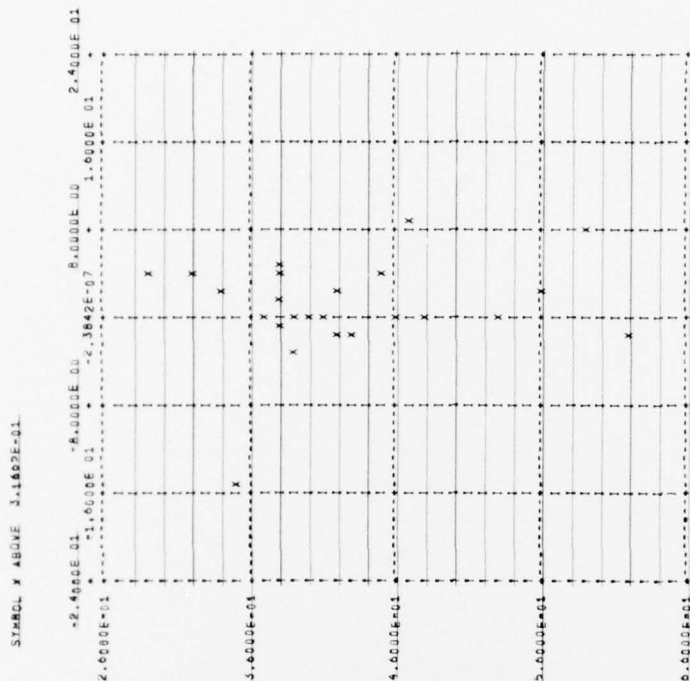Figure 36.   RFM Pulse with Multipath, RVI Display, 3-db Threshold

Figure 37.   RFM Pulse with Multipath, RVI Display, 6-db Threshold

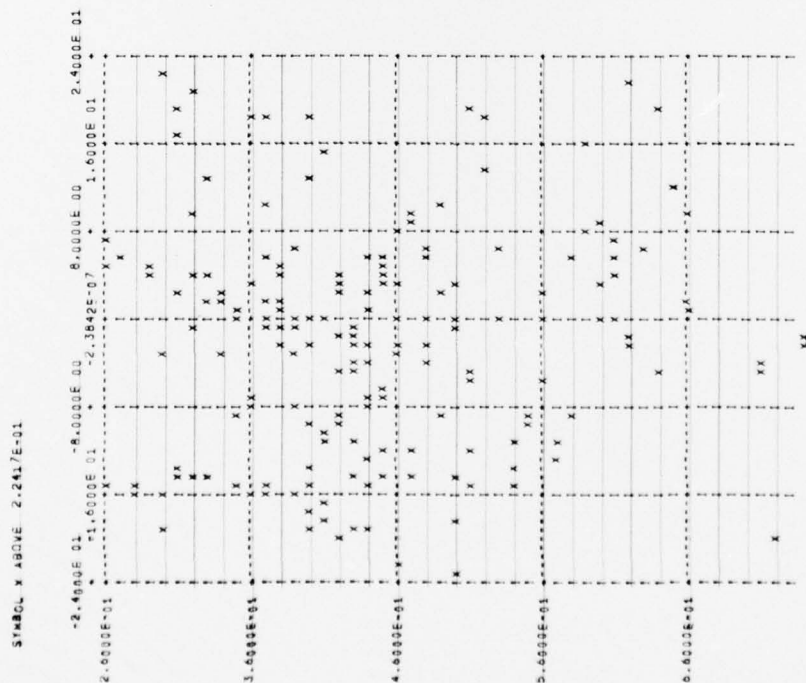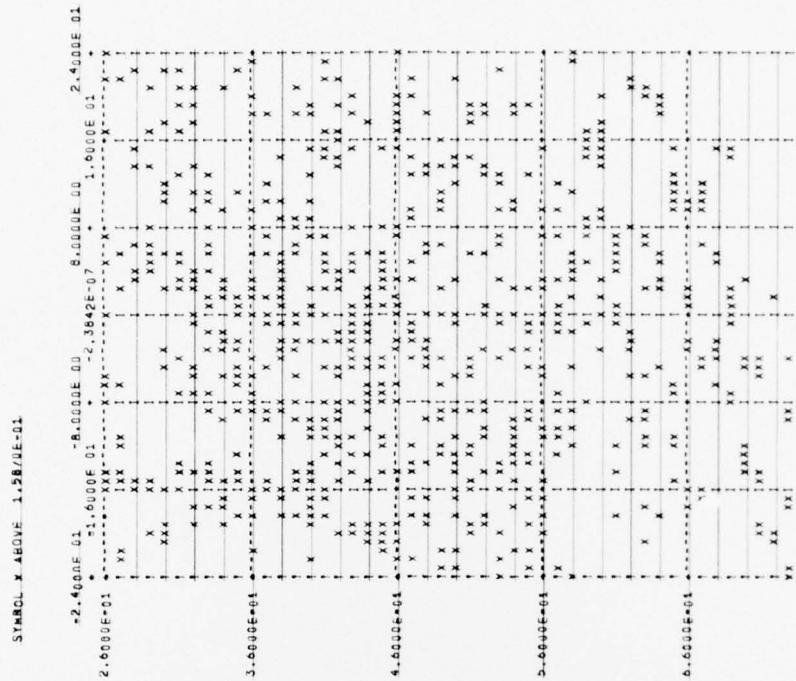Figure 38.   RFM Pulse with Multipath, RVI Display, 9-db Threshold

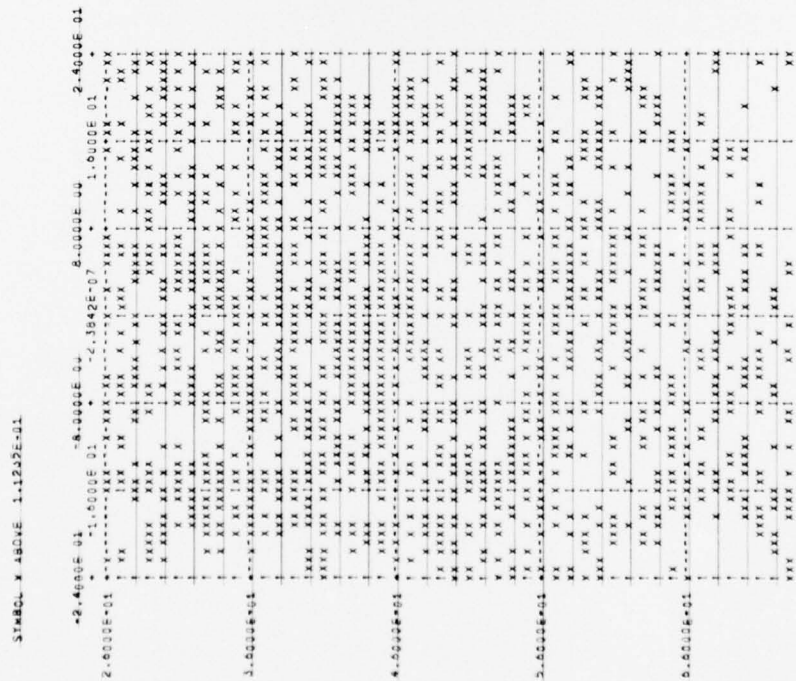Figure 39. RFM Pulse with Multipath, RVI Display, 12-db Threshold

Figure 40. RFM Pulse with Multipath, RVI Display, 15-db Threshold

V. CONCLUDING REMARKS

The results obtained by the simulation procedure described in Section IV sppear to be quite significant. The RVI displays of Figures 31 through 40 are agonizingly familiar to those who have studied the sea data analysis.* On the basis of the signal processing being employed, an operator viewing such displays has no choice but to announce that there are a multiplicity of targets present at a variety of ranges and dopplers. If only a single target is known to be present, then the displays have little physical significance. The latter case is, of course, more nearly correct; the RVI displays of Figures 31 through 40, and their counterparts in the previous report, have little physical significance in terms of actual target behavior.

Consider the following explanation. Waveforms having high BT products such as PRN and RFM offer, in theory at least, excellent resolution in both range and doppler. Unfortunately, the theory of ambiguity functions also reveals that the volume under the normalized ambiguity surface is a constant regardless of the waveform employed. It then follows that if the central spike of the ambiguity function is narrow in both range and doppler, the volume within this spike will be small. The skirts of such ambiguity functions must, as a consequence, contain the bulk of the volume. The successful use of "thumbtack" waveforms such as PRN and RFM, therefore, is predicated on the absence of multipath. In a multipath situation the ambiguity skirts of the individual multipath components tend to add on a random basis, and the response in certain skirt regions approaches or even exceeds the response of the main peaks corresponding to the various paths. Thus multipath tends to produce the flooding of the RVI displays that has been observed both in this report and in the sea data analysis of the previous report.

It should be pointed out again (as mentioned several times in the previous report) that computer analysis of sea data implies a significant advantage which cannot be realized in practice. This involves the precise setting of the threshold level of the RVI displays. The computer searches all values representing the RVI display and finds the largest value; the threshold is then set relative to this largest value. Such precise operation is hardly possible under operational conditions. The displays shown in this report and also in the previous report, poor as they may be, imply the use of this significant advantage which would be unavailable in practice. Thus it becomes rather obvious that

system performance using any waveform which has good resolution in both range and doppler will suffer considerably if multipath effects are encountered. Any significant amount of multipath will quickly flood the RVI displays and the information obtained from such displays becomes meaningless.

There is often a temptation to classify waveforms only on the basis of their bandwidth-time produce; this is sometimes misleading -- the FM waveform discussed in this report is a good case in point. This waveform has the same BT product as the PRN and RFM waveforms, yet FM behaved quite well with regard to the RVI displays from a detection standpoint only. Of course, FM cannot resolve the range-doppler ambiguity and in this case FM is in a different class than the PRN and RFM waveforms. The volume under the ambiguity surface in the FM case is well-confined to the region under the main ridge, as was noted in both this and the previous report. As a consequence, use of this waveform does not produce the RVI flooding under multipath conditions which was encountered in the PRN and RFM cases, and this characteristic of FM enhances the detection performance of the system.

The results obtained in this simulation study are believed to answer many of the questions that were raised in the previous report when actual sea data was analyzed. It must not be concluded, however, that multipath is the only adverse mechanism involved in the sea returns; there may well be other mechanisms contributing to performance degradation. What has been shown in this report is that multipath alone can produce many of the anomalous results which were observed in the sea data for the RFM and PRN returns.

By way of further conjecture, some additional operating results which have been reported might be discussed at this point. The PRN mode of operation of the AN/SQS-26 system has apparently given very poor results. In light of the present data this experience is not at all surprising. First, let us consider that PRN modulation is being used at sea but that an analog correlator is available in the signal processor lineup. An operator, viewing RVI displays such as the ones simulated here, might be alerted to the presence of a target on the basis that his display became more active in a particular portion of the range sweep. This activity would no doubt result in a flooded presentation if multipath were present. The operator might be aware of the presence of a target even though the display would tell him nothing about the precise range or doppler of such a

target. In a sense the complex processor and display just described is being used by the operator as a simple energy detector -- there are easier ways of accomplishing this.

In practice, an analog correlator is not employed in the AN/SQS-26 system -- a Deltic correlator is used. The Deltic correlator employs hard limiting and, as a consequence, it would be doubtful that an operator viewing an RVI display connected to a Deltic correlator would be alerted to a PRN-multipath return. The Deltic normalization would tend to prevent the scope from looking "busier" during the target interval as compared to other intervals. As was stated previously, this represents conjecture but in view of the results obtained this seems to be a reasonable conjecture.

The conclusion reached in the previous report -- that the operational environment of the AN/SQS-26 does not permit accurate range and doppler information to be obtained from a single pulse -- still stands. Furthermore, there is now sufficient reason to suspect that attempts to obtain target range and velocity accurately from pulses of a single type will not only fail in reaching that goal but may also result in loss of target detectability.

Some serious thought should be given to the choice of waveforms which are compatible with the operating environment. For example, if future tests indicate consistent multipath spreads on the order of, say, 100 to 200 msec, is anything to be gained by using a waveform which has 10-msec resolution? There is every indication that not only is there nothing to be gained by such a mismatch, but much may be lost in the process. The same situation holds, of course, in the frequency domain. If a doppler spread exists which is inherent in the environment, then it does not seem appropriate to use waveforms which can resolve doppler to some fraction of this environmental doppler spread. Case in point: FM gives neither accurate range nor doppler information, yet it is known from experience that this waveform does the best job of detecting targets in reverberation. Maybe nature is trying to tell us something.